# IDŐJÁRÁS

QUARTERLY JOURNAL
OF THE HUNGARIAN METEOROLOGICAL SERVICE

CONTENTS



VOL. 99 * NO. 1 * JANUARY–MARCH 1995

# IDŐJÁRÁS

*Quarterly Journal of the Hungarian Meteorological Service*

*Editor-in-Chief*
**G. MAJOR**

*Editor*
**T. TÄNCZER**

*Technical Editor*
**Ms. M. ANTAL**

**EDITORIAL BOARD**

*AMBRÓZY, P. (Budapest)*
*ANTAL, E. (Budapest)*
*BOTTENHEIM, J. (Downsview, Ont)*
*CZELNAI, R. (Budapest)*
*DÉVÉNYI, D. (Boulder, CO)*
*DRĂGHICI, I. (Bucharest)*
*FARAGÓ, T. (Budapest)*
*FISHER, B. (London)*
*GEORGII, H.-W. (Frankfurt a. M.)*
*GÖTZ, G. (Budapest)*
*HASZPRA, L. (Budapest)*
*IVÁNYI, Z. (Budapest)*
*KONDRATYEV, K.Ya. (St. Petersburg)*
*MÉSZÁROS, E. (Veszprém)*
*MÖLLER, D. (Berlin)*
*NEUWIRTH, F. (Vienna)*
*PANCHEV, S. (Sofia)*
*PRÁGER, T. (Budapest)*
*PRETEL, J. (Prague)*
*RÁKÓCZI, F. (Budapest)*
*RENOUX, A. (Paris-Créteil)*
*SPÄNKUCH, D. (Potsdam)*
*STAROSOLSZKY, Ö. (Budapest)*
*VALI, G. (Laramie, WY)*
*VARGA-HASZONITS, Z. (Mosonmagyaróvár)*
*WILHITE, D. A. (Lincoln, NE)*
*ZÁVODSKÝ, D. (Bratislava)*

*Editorial Office: P.O. Box 39, H–1675 Budapest, Hungary*

*Subscription from customers in Hungary should be sent to the Financial Department of the Hungarian Meteorological Service Kitaibel Pál u. 1, 1024 Budapest. The subscription rate is HUF 2500.*

*Abroad the journal can be purchased from the distributor: KULTURA, P.O. Box 149, H–1389 Budapest. The annual subscription rate is USD 55.*

# IDŐJÁRÁS

*Quarterly Journal of the Hungarian Meteorological Service*
*Vol. 99, No. 1, January–March 1995*


# Predictability of nonlinear dynamical systems


**G. Götz**

*Lupény utca 6-8, H-1026 Budapest, Hungary*



*(Manuscript received 22 December 1994; in final form 30 January 1995)*



**Abstract**—One of the basic tenets of science is that deterministic systems are predictable: given the initial condition and the equations describing a system, the behaviour of the system can be predicted for all time. The recent discovery of chaotic systems has eliminated this viewpoint. A chaotic system is a deterministic system that exhibits aperiodic behaviour. Another property of a chaotic system is sensitive dependence on initial conditions. Therefore, no matter how precisely the initial conditions are known, the long-term behaviour of a chaotic system can never be predicted. Chaos can readily occur in all dynamical systems where nonlinearity is present: the required dimensionality of the system is only three for autonomous continuous-time systems, two for invertible discrete-time systems, and one for noninvertible discrete-time systems.

Following a short historical review of the problem of predictability, we outline some quantitative measures of chaotic behaviour: the Lyapunov exponents, the metric entropy, and fractal dimensions. We show that the predictability problem is intrinsically linear in its early stages; nonlinearity affects the evolving basic state that is perturbed and ultimately it also affects the saturation of the perturbation growth. Yet, for sufficiently small perturbations there is an interval in which the tangent linear equations are valid.

Dynamical systems theory has provided a new quantitative perspective on the predictability of weather and climate processes. The analysis of model-generated and observational time series confirmes the existence of intrinsically imposed limits of atmospheric predictability. Introduction of ensemble forecast techniques is an explicit recognition that the atmosphere exhibits random behaviour. At the end of this review article, the basic concept of ensemble prediction is outlined with special emphasis on the selection of optimal perturbations.



*Key-words*: chaos, Lyapunov exponents, metric entropy, fractal dimensions, ensemble prediction.


## *1. Introduction*

The question of *predictability* has a long history in physics. Following the formulation of the classical deterministic laws of mechanics by Isaac Newton in the 17th century, many scientists had a fundamental belief that once one had

determined the laws governing the Universe, it was just a matter of solving the equations, with appropriate starting conditions, to discover its past and future behaviour. The most extreme form of this doctrine was strikingly expounded by Pierre Simon de Laplace in the 19th century. He envisaged a supreme intelligence in his *Essai philosophique sur les probabilités* (1814): 'Such an intelligence would embrace in the same formula the movements of the greatest bodies of the Universe and those of the lightest atom; for it, nothing would be uncertain and the future, as the past, would be present to its eyes.'

Then, in the 1920s, quantum mechanics came along. At the heart of quantum physics lies Heisenberg's uncertainty principle, which states that it is impossible to determine with accuracy both the position and the momentum of a particle, and therefore everything we can measure is subject to truly random fluctuations. Quantum fluctuations are not the result of human limitations or hidden degrees of freedom; they are inherent in the working of nature on atomic scales. Quantum mechanics has thus introduced *probability* and *randomness*, i.e. an element of *genuine unpredictability* at a fundamental level into physics, that greatly upset Albert Einstein: 'God does not play dice', he said.

Then, surprisingly, the modern study of nonlinear dynamical systems from the 1960s has shown us that even the classical Newtonian physics has randomness and unpredictability at its core. Numerical simulations — playing a crucial role in the process of finding and analysing nonlinear phenomena, and becoming more and more wide-spread with the recent availability of digital computing power — have revealed that deterministic systems may exhibit random behaviour.[1] We now know that such a strange behaviour, also called *chaos*, can readily occur in all systems where *nonlinearity* is present. Indeed, chaos has been reported from virtually every scientific discipline, including even mathematics: there are theorems connected with the most traditional branch of pure mathematics, number theory, that cannot be proved because when we ask questions, we obtain results that are equivalent to the random toss of coin.

There is no generally accepted definition of chaos. We know that a chaotic spectrum is not composed solely of discrete frequencies, but has a continuous, broad-band nature. We also know that the attracting limit set for chaotic behaviour is not a simple geometrical object like a circle or a torus, but is related to fractals and Cantor sets. Another property of chaotic systems is *sensitive dependence on initial conditions*: given two different initial conditions arbitrarily close to one another, the phase-space trajectories emanating from these points diverge at a rate characteristic of the system until, for all practical purposes, they are uncorrelated. This divergence is determined by the system's internal dynamical instabilities associated with the part of the phase space

---

[1]There are random events in nature, but science has typically used *probabilistic* models to describe them.

through which the trajectories evolve. In practice, the initial state of a system can never be specified exactly, but only to within some tolerance $\epsilon(0) > 0$; if two initial conditions $x_1(0)$ and $x_2(0)$ lie within $\epsilon(0)$ of one another, they cannot be distinguished. However, after a finite amount of time, $x_1(t)$ and $x_2(t)$ will diverge and become unrelated (*Fig. 1*). Therefore, no matter how precisely the initial condition is known, the long-term behaviour of a chaotic system can never be predicted. (Of course, in theory, if the initial condition could be specified to infinite precision, the phase-space trajectory of a mathematical dynamical system could be predicted precisely.)

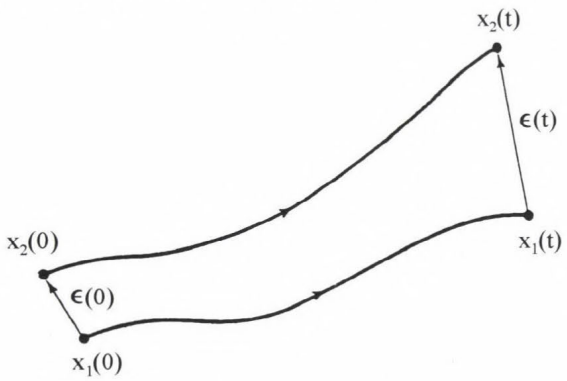


*Fig. 1.* Evolution of two nearby trajectories in phase space.

It should be noted that there were classical physicists and mathematicians, even in the previous century, who had thought about nonlinear dynamical systems. Jacques Hadamard first observed the sensitivity of solutions to initial conditions at the end of the last century in a rather specific system called geodesic flow. Subsequently, J. Henri Poincaré discussed in 1908 sensitivity to initial conditions and unpredictability at the level of scientific philosophy. Poincaré even went on to discuss the problem of weather predictability. However, their ideas seem to have been forgotten until *Lorenz* (1963) rediscovered them independently in his elegant paper more than half a century later.

It is quite understandable that in the meanwhile atmospheric scientists have focussed their attention mainly on looking for attainable methods of predicting the weather. It became soon obvious that no simple set of causal relationships can be found which relate the state of the atmosphere at one instant of time to its state at another. It was this realization that led *Vilhelm Bjerknes* (1904) to define the *theoretical* problem of prognosis in terms of the Newtonian physics: 'If it is true, as every scientist believes, that subsequent atmospheric states develop from the preceding ones according to physical laws, then it is apparent that the necessary and sufficient conditions for the rational solution of the forecasting problem are the following: (1) A sufficiently accurate knowledge of

the state of the atmosphere at the initial time. (2) A sufficiently accurate knowledge of the laws according to which one state of the atmosphere develops from another.'

But it remained for *Lewis F. Richardson* (1922) to suggest the *practical* means for the solution of this problem: he proposed to integrate the equations of motion *numerically,* and showed how this might be done. That the actual forecast used to test his method was unsuccessful was in no sense a measure of the value of his work. Then, for a long time, no one ventured to follow Richardson's footsteps. It was only 25 years later, with the increase in density and extent of the observational network on the one hand, and the development of high-speed computing machines on the other, that an international meteorological working group at the Institute for Advanced Study in Princeton, New Jersey could adopt a general plan of attacking the problem of numerical weather prediction by a step by step investigation of a series of simplified models of the atmosphere (*Charney et al.*, 1950; *Charney*, 1951).

Questions of predictability were not in the forefront of interest in those days, although O. G. Sutton warned in 1951 that the weather problem might be inherently unsolvable because of very small random influences having great effects within unstable systems in the atmosphere. In 1953, P. Raethjen considered the atmosphere nearly always to be in the situation of 'a Hercules at the cross-roads'. He pointed out that even minute influences may suffice to change a stable atmosphere into an unstable one when the state passes a certain threshold value; and then a 'decision' with fundamental consequences may in its turn be triggered. 'The manifold instability of the atmosphere will always remain an invincible hindrance to a physically founded and exact weather forecasting,' Raethjen said (see *Bergeron*, 1959).

The words *classical predictability studies* now usually refer to those works in which an attempt is made to arrive at a qualitative estimate of the growth rate of an individual error and to determine the limits of predictability. In these studies, either simple models of the atmospheric flow or complex models of the general circulation of the atmosphere with explicit treatments of thermal and mechanical forcings are used. The first such study reported in the literature is the one by *Thompson* (1957) who showed, using a simple barotropic model, that the initial errors tend to grow with time and that the atmospheric flow is not predictable beyond a week. A review of the subsequent attempts to determine the limits of atmospheric predictability along this line can be found in the article by *Shukla* (1985).

The recent (within the last twenty-five years) discovery of chaotic systems has given birth to a rapidly developing interdisciplinary field of research called *nonlinear dynamics*. The investigation of the inherent forecasting limitation in fluid-flow problems is currently one of the most exciting topics in nonlinear systems research. The purpose of this paper is to look over the new quantitative perspective on predictability provided by dynamical systems theory and to

illustrate how the numerical weather prediction problem can be handled in the light of the new findings.

## 2. *Quantitative measures of chaos*

Considering the question of the required dimensionality of a system for chaos, we must distinguish between discrete-time dynamical systems and dynamical systems in which time is a continuous variable. A *discrete, integer-valued* time dynamical system is defined by the state equation

$$\mathbf{x}_{k+1} = \mathbf{M}(\mathbf{x}_k), \tag{1}$$

where $k$ denotes the time variable ($k = 0,1,2,\ldots$), the state $\mathbf{x}$ is an $n$-dimensional vector $\mathbf{x}_k = (x_k^{(1)}, x_k^{(2)}, \ldots, x_k^{(n)})$, and $\mathbf{M}$ maps the state $\mathbf{x}_k$ to the next state $\mathbf{x}_{k+1}$. If the map $\mathbf{M}$ is noninvertible, i.e. if given $\mathbf{x}_{k+1}$, we cannot solve Eq. (1) for $\mathbf{x}_k$, chaos is possible even in one-dimensional maps. A famous example is the logistic map $x_{k+1} = rx_k(1 - x_k)$, which exhibits chaos for large enough control parameter $r$. If the map $\mathbf{M}$ is invertible, there can be no chaos unless $n \geq 2$.

An example of a dynamical system in which time $t$ is a *continuous* variable is a system of $n$ first-order ordinary differential equations, which we can write in vector form as

$$d\mathbf{x}/dt = \mathbf{f}(\mathbf{x}), \tag{2}$$

where $\mathbf{x}$ is again an $n$-dimensional state vector, and since the vector field $\mathbf{f}$ does not depend on time, Eq. (2) defines an autonomous dynamical system. It is common to refer to a continuous-time dynamical system as a *flow*. In the case of (2), $n \geq 3$ is the sufficient condition for chaos to be possible. For example, according to the Poincaré-Bendixon theorem, the only possible attracting solutions of (2) for $\mathbf{x}$ a two-dimensional vector in the phase plane are periodic solutions, steady states and solutions in which the phase-plane trajectory approaches a figure '8' or one of its lobes; in all these cases, the behaviour of the system is not chaotic (*Hirsch* and *Smale*, 1974).

In order to make the notion of 'sensitive dependence on initial conditions' quantitative, different measures have been introduced. A concise survey of these measures is the subject of the following subsections; for a more detailed discussion, the reader is referred to the work by *Ott* (1993).

### *2.1 Error growth and Lyapunov exponents*

The mathematical formulation of sensitivity to initial conditions, entailing the growth of small initial perturbations (errors), has been provided by *Oseledec*

(1968). Oseledec's multiplicative ergodic theorem guarantees the existence of a *globally averaged* rate of exponential divergence under very general circumstances; it is referred to as the (largest) *Lyapunov exponent* and is an invariant of the whole dynamical system (see, for example, *Ruelle*, 1989).

Let $\mathbf{x}(0)$ be an initial condition at time 0 and $\mathbf{x}(t)$ the corresponding solution to the real $n$-dimensional dynamical system (2) for $t > 0$. If we consider an infinitesimal departure from the initial condition $\mathbf{x}(0)$ denoted by $\delta\mathbf{x}(0)$ then, according to the linear stability theorem, the temporal evolution of this initial perturbation is approximately governed by the linearized counterpart of Eq. (2) which can be written as

$$\frac{d}{dt}\delta\mathbf{x}(t) = \boldsymbol{J}(t) \cdot \delta\mathbf{x}(0)\,. \tag{3}$$

Here $\boldsymbol{J}(t)$ denotes the $n \times n$ Jacobian matrix of the partial derivatives of $\mathbf{f}(\mathbf{x})$ evaluated at some time $t$ with respect to the initial condition $\mathbf{x}(0)$:

$$\boldsymbol{J}(t) = \begin{bmatrix} \dfrac{\partial f^{(1)}}{\partial x^{(1)}} & \dfrac{\partial f^{(1)}}{\partial x^{(2)}} & & \dfrac{\partial f^{(1)}}{\partial x^{(n)}} \\ \dfrac{\partial f^{(2)}}{\partial x^{(1)}} & \dfrac{\partial f^{(2)}}{\partial x^{(2)}} & \cdots & \dfrac{\partial f^{(2)}}{\partial x^{(n)}} \\ & \vdots & & \\ \dfrac{\partial f^{(n)}}{\partial x^{(1)}} & \dfrac{\partial f^{(n)}}{\partial x^{(2)}} & & \dfrac{\partial f^{(n)}}{\partial x^{(n)}} \end{bmatrix},$$

i.e. one can write Eq. (3) in the scalar form as

$$\frac{d}{dt}\delta x^{(i)} = \sum_{j=1}^{n} \frac{\partial f^{(i)}}{\partial x^{(j)}}\,\delta x^{(j)} \quad (i = 1,2,\ldots,n)\,, \tag{4}$$

in which the coefficients $\partial f^{(i)}/\partial x^{(j)}$ are in general a function of time. The linear system of equations (3) is called the *tangent linear system* of (2) in the vicinity of the basic state $\mathbf{x}(t)$.

Integrating Eq. (3) over some portion of the phase-space trajectory $\mathbf{x}$ between times 0 and $t$, we obtain

$$\delta \mathbf{x}(t) = \boldsymbol{A}(t) \cdot \mathbf{x}(0), \tag{5}$$

where the $n \times n$ linear operator $\boldsymbol{A}(t)$ is the matrix solution of the equation $d\boldsymbol{A}/dt = \boldsymbol{J} \cdot \boldsymbol{A}$ subject to the initial condition $\boldsymbol{A}(\mathbf{x}(0),0) = \boldsymbol{I}$ ($\boldsymbol{I}$ denoting the $n \times n$ identity matrix). Thus, $\boldsymbol{A}(t)$ depends upon the values of $\mathbf{x}$ between times 0 and $t$, and controls the growth of small perturbations during this time interval. Therefore, the evolution operator $\boldsymbol{A}$ is often referred to as the *error matrix*. If the variations in the basic state between times 0 and $t$ are neglected, so that $\boldsymbol{J}(t)$ is constant, one can write

$$\boldsymbol{A}(t) = e^{\boldsymbol{J}(t)}. \tag{6}$$

We call the vectors $\delta \mathbf{x}(t)$ *tangent vectors* of the system, and the space in which they lie the *tangent space* to $\mathbf{x}(t)$. Eq. (5) describes the sum of all perturbations that are of normal-mode form. In general, the $n$ eigenvalues of the matrix $\boldsymbol{A}$ are either real or else occur in complex conjugate pairs. The normal modes in (5) are, therefore, growing, decaying, or oscillatory depending on the type of the $i$th eigenvalue. Furthermore, due to the possible asymmetry of the Jacobian $\boldsymbol{J}(t)$, which is always the case for realistic basic-state flows, the eigenvectors of $\boldsymbol{A}$ are not necessarily orthogonal to each other, a fact that has an important impact on the initial evolution of small perturbations, as it will be discussed in Section 3.

Let us now consider the evolution of the initial departures (errors) on the surface of an $n$-dimensional hypersphere with a radius of $\epsilon$:

$$\delta \mathbf{x}^{\mathrm{T}}(0) \cdot \delta \mathbf{x}(0) = \epsilon^2, \tag{7}$$

where T denotes the transpose of a matrix. As each error in the ensemble is allowed to evolve according to Eq. (5), this sphere will be deformed at time $t$ into an ellipsoid given by

$$\delta \mathbf{x}^{\mathrm{T}}(t) \, [\boldsymbol{A}(t) \cdot \boldsymbol{A}^{\mathrm{T}}(t)]^{-1} \, \delta \mathbf{x}(t) = \epsilon^2. \tag{8}$$

Whilst in general $\boldsymbol{A}(t)$ is not symmetric, by construction the product operator $\boldsymbol{A}(t) \cdot \boldsymbol{A}^{\mathrm{T}}(t)$ is, and possesses $n$ real non-negative eigenvalues. If these are denoted by $\gamma_i^2(t)$ and ordered such that $\gamma_1^2(t) \geq \gamma_2^2(t) \geq \ldots \geq \gamma_n^2(t)$, then the principal axes of the error ellipsoid at time $t$ will be $\epsilon\gamma_1, \epsilon\gamma_2, \ldots, \epsilon\gamma_n$. Thus $\gamma_i$, which are by definition the singular values of the error matrix $\boldsymbol{A}$, correspond

to the factors by which the components of an infinitesimal deviation $\delta\mathbf{x}(0)$ from the initial condition $\mathbf{x}(0)$ grow ($\gamma_i > 0$) or shrink ($\gamma_i < 0$) in the phase space parallel to the respective orthogonal singular vectors of $\boldsymbol{A}$. In other words, the fastest growing perturbations are the eigenvectors belonging to the largest eigenvalues of the product operator $\boldsymbol{A} \cdot \boldsymbol{A}^{\mathrm{T}}$.

If the limits

$$l_i = \lim_{t\to\infty} \left[\gamma_i(t)\right]^{1/t} \qquad (i = 1,2,\ldots,n) \tag{9}$$

exist, and the positive $t$th root is taken, these quantities are called *Lyapunov numbers*, while

$$\lambda_i = \ln l_i = \lim_{t\to\infty} \left\{\ln\left[\gamma_i(t)\right]^{1/t}\right\} \qquad (i = 1,2,\ldots,n) \tag{10}$$

define the *Lyapunov exponents* for the initial condition $\mathbf{x}(0)$ and the orientation of the initial perturbation $\delta\mathbf{x}(0)/|\delta\mathbf{x}(0)|$. Eq. (10) can also be expressed in the form

$$\lambda_i = \lim_{t\to\infty} \frac{1}{t} \ln \frac{\delta x^{(i)}(t)}{\delta x^{(i)}(0)} \qquad (i = 1,2,\ldots,n). \tag{11}$$

The ordered set $\lambda_1 \geq \lambda_2 \geq \ldots \geq \lambda_n$ gives the spectrum of Lyapunov exponents of the $n$th-order dynamical system. This spectrum is an invariant of the system, independent of the trajectory, except for a set of initial conditions of Lebesgue measure zero (*Parker* and *Chua*, 1987).

In the case of discrete-time dynamical systems (1), all the above considerations carry through with the linearized evolution of the infinitesimal departure from $\mathbf{x}_0$ in the direction of the tangent vector $\delta\mathbf{x}_0$ determined now by

$$\delta\mathbf{x}_{k+1} = \mathbf{DM}(\mathbf{x}_k) \cdot \delta\mathbf{x}_k, \tag{12}$$

where $\mathbf{DM}(\mathbf{x}) = \partial\mathbf{M}(\mathbf{x})/\partial\mathbf{x}$ is a Jacobian matrix. From Eq. (12), we have

$$\delta\mathbf{x}_k = \mathbf{DM}^k(\mathbf{x}_0) \cdot \delta\mathbf{x}_0, \tag{13}$$

where

$$\mathbf{DM}^k(\mathbf{x}_0) = \mathbf{DM}(\mathbf{x}_{k-1}) \cdot \mathbf{DM}(\mathbf{x}_{k-2}) \cdot \ldots \cdot \mathbf{DM}(\mathbf{x}_0),$$

i.e. $\mathbf{DM}^k$ plays the roles of $\boldsymbol{A}(t)$ in Eq. (5) in the treatment of continuous-time systems, and Eq. (11) is now replaced by

$$\lambda_i = \lim_{k\to\infty} \frac{1}{k} \ln \frac{\delta x_k^{(i)}}{\delta x_o^{(i)}} \qquad (i = 1,2,\ldots,n)\,. \tag{14}$$

From Eqs. (11) and (14) it follows that

$$\delta x^{(i)}(t) \sim \delta x^{(i)}(0)\, e^{\lambda_i t} \tag{15}$$

and

$$\delta x_k^{(i)} \sim \delta x_o^{(i)} e^{\lambda_i k}, \tag{16}$$

i.e., the Lyapunov exponents characterize the temporally averaged (global) exponential rate of divergence ($\lambda_i > 0$) or convergence ($\lambda_i < 0$) of infinitesimally nearby initial states. If $|\delta\mathbf{x}(t)| > |\delta\mathbf{x}(0)|$ for any $t > 0$, the continuous-time system is called *expanding flow*. Thus, positive Lyapunov exponents quantify the long time expansion occurring in a dynamical system. The inverse of the sum of the positive Lyapunov exponents $(\Sigma\lambda_+)^{-1}$ gives an estimate of the mean $e$-folding time $t_e$ of the initial growth of infinitesimal errors, which is usually looked upon as the deterministic predictability time of the system. (For predictability experiments, the common measure is the mean doubling time $t_d$ of small errors, which is obtained by $(\Sigma\lambda_+)^{-1} \ln 2$.) In this way, positive Lyapunov exponents are a quantitative measure of the average degree of sensitive dependence on initial conditions of the system, or equivalently, the average exponential rate at which deterministic predictive ability is lost.

The sum of the Lyapunov exponents is the average divergence of the flow. For bounded hydrodynamical systems, forcing and quadratic dissipation combine to restrict all trajectories to a closed region of the phase space, i.e., contraction of phase-space volumes outweighs expansion, so

$$\sum_{i=1}^{n} \lambda_i < 0\,. \tag{17}$$

Thus at least one exponent is negative, and the post-transient motion of trajectories eventually occurs on a zero-volume invariant subset of the phase space, the *system attractor*.

For an illustrative example, we consider a two-dimensional map **M** and sprinkle initial conditions isotropically in a sufficiently small error circle of radius $\epsilon(0)$ around $\mathbf{x}_o$. We suppose that the system is characterized by $\lambda_1 > 0$ ($l_1 > 1$) and $\lambda_2 < 0$ ($l_2 < 1$), and each initial condition evolves under the map **M**.

In this case, $k$ iterations of the map transform the initial error circle approximately into an ellipse with amplifying major radius $\epsilon(0)e^{\lambda_1 k} = \epsilon(0)l_1^k$, representing an unstable direction, and decaying minor radius $\epsilon(0)e^{\lambda_2 k} = \epsilon(0)l_2^k$, which represents a stable direction in the phase space (*Fig. 2*).

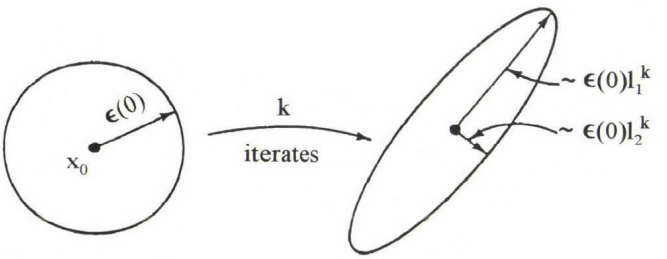


*Fig. 2.* Evolution of an initially infinitesimal error ball in phase space after $k$ iterations of the map.

If an initial state $\mathbf{x}(t_0)$ and hence $\mathbf{x}(t)$ are on the attractor, the limits in Eq. (10) may be replaced by limits as the initial time $t_0 \to -\infty$ while $t$ remains fixed. Unit vectors $\mathbf{L}_i$ ($i = 1,2,\ldots,n$) parallel to the principal axes of the error ellipsoid (8) may also approach limits as $t_0 \to -\infty$. In this case these limits are called the *Lyapunov vectors* at $\mathbf{x}(t)$. As it was shown by *Lorenz* (1984a), hypersurfaces on an attractor extend in the expanding, neutral and contracting local directions of $\mathbf{L}_i$ with positive, zero and negative exponents, respectively.

Lyapunov exponents are convenient for categorizing the consolidated final-state behaviour of dynamical systems. For stable constant solutions, $\lambda_i < 0$ for all $i$; for stable periodic solutions, $\lambda_1 = 0$ and $\lambda_i < 0$ for $i = 2,3,\ldots,n$; for a two-periodic solution, $\lambda_1 = \lambda_2 = 0$ and $\lambda_i < 0$ for $i = 3,4,\ldots,n$; and for a $K$-periodic solution, $\lambda_1 = \lambda_2 = \ldots = \lambda_K = 0$ and $\lambda_i < 0$ for $i = K + 1, K + 2,\ldots,n$. The behaviour of these systems is predictable in that small errors in specifying a state point on the respective attractor (fixed point, limit cycle, $K$-torus) remain constant or decrease over long times. What distinguishes a *chaotic* system from these classical, well-behaved types of deterministic dynamical systems is the existence of at least one *positive* Lyapunov exponent. In the three-dimensional case, $\lambda_1 > 0$, $\lambda_2 = 0$ and $\lambda_3 < 0$. In four-dimensional and higher-dimensional systems, the case of more than one positive Lyapunov exponent has been termed *hyper-chaos*, since there is expansion on the chaotic, or strange attractor in more than one phase-space direction.

We close this subsection by noting that since the Lyapunov exponents are defined in the limit as $t \to \infty$, any finite transient may be neglected and,

therefore, every point in the basin of attraction of an attractor has the same Lyapunov exponents as the attractor. On the other hand, initially nearby trajectories need not diverge at the same rate on *all* parts of a chaotic attractor (*Benzi* and *Carnevale*, 1989). This variability of the *local* divergence rate in phase space can result from the proximity of trajectories to unstable fixed points and unstable manifolds. Clearly, whereas the Lyapunov exponents quantify global, or time-averaged predictability of the flow, the local divergence rates measure the instantaneous predictability as a function of phase-space position (*Abarbanel et al.*, 1991).

If time is written as $t = k\tau$ ($k = 0,1,2,\ldots$), where $\tau$ is the time step of the model, then a local divergence rate can be defined as

$$D[\mathbf{x}(k\tau)] = \frac{1}{\tau} \ln \frac{|\delta\mathbf{x}[(k+1)\tau]|}{|\delta\mathbf{x}(k\tau)|}. \tag{18}$$

The largest of the $n$ local divergence rates $D_{\max}$ measures local predictability at the phase-space point $\mathbf{x}$ on a time scale equal to $\tau$, and $1/D_{\max}$ approximates the $e$-folding time of local error growth (*Nese*, 1989). This quantity may vary significantly on the attractor, producing alternating periods of enhanced and limited predictability. The averaged $\bar{D}_{\max}$ of $D_{\max}(t)$ over a trajectory is at least $\lambda_1$. The fact that $\bar{D}_{\max} \geq \lambda_1$, rather than $\bar{D}_{\max} = \lambda_1$, is due to the difference between the two definitions (18) and (11); for a more detailed mathematical explanation, see *Legras* and *Ghil* (1985).

Another measure of the local error growth rate can be defined directly from the eigenvalues $\gamma_i^2$ of the matrix $\boldsymbol{A}(t) \cdot \boldsymbol{A}^{\mathrm{T}}(t)$ appearing in Eq. (8):

$$\Lambda(t) = \left[\frac{1}{n} \sum_{i=1}^{n} \gamma_i^2(t)\right]^{1/2}, \tag{19}$$

which was introduced by *Lorenz* (1965), and therefore it is often referred to as the *Lorenz index*. $\Lambda(t)$ gives the ensemble average of the linear growth rate of infinitesimally small initial root-mean-square errors. This index depends neidher on the amplitude nor the configuration of the initial perturbation, but directly represents the local instability characteristics of the flow (*Mukougawa et al.*, 1991).

When differential equations are replaced by integral equations along a trajectory for estimating the linear perturbations that have the fastest growth over some finite trajectory segment, the role of the error matrix in Eq. (5) is taken over by an integral propagator operator $\boldsymbol{R}(t_1,t_2)$ of the linearized equations of the dynamical system, integrated between times $t_1$ and $t_2$. The divergence

rates for finite segments of a trajectory are given by the singular values of $\boldsymbol{R}$, which are equivalent to the eigenvalues of the product operator $\boldsymbol{R}^*\boldsymbol{R}$, where * denotes the adjoint operation. The corresponding phase-space directions associated with the divergence rates are the singular vectors of $\boldsymbol{R}$, equivalent to the eigenvectors of $\boldsymbol{R}^*\boldsymbol{R}$. For very long time intervals $(t_2 - t_1) \to \infty$, the eigenvalues of $\boldsymbol{R}^*\boldsymbol{R}$ become equal to the Lyapunov exponents associated with the attractor (*Zeng*, 1991; *Buizza et al.*, 1992; *Palmer*, 1993). (Note that because of its very nature, an adjoint operation proceeds from the output of the model at time $t_2$ to its input at time $t_1$, which means that the governing equations must be integrated *backwards* in time. Theoretical and numerical problems of integrating adjoint models are mainly related to irreversible physical processes; the details of these problems are beyond the scope of the present paper.)

### 2.2 *The metric entropy*

Suppose that the state of the system can be measured to within a resolution of $\epsilon$. Assume there are two observers who measure the state of the system at two different times. Observer 1 observes the state at time $t_1$ to be $x_1$. Observer 2 measures the state at time $t_2 > t_1$ to be $x_2$. Which observer knows more about the state of the system, observer 1 or 2?

As we saw in Section 2.1, a chaotic system expands in some directions in the phase space, and the predictive value of the initial condition deteriorates with time. Therefore, it is more accurate to observe the state at time $t_2$ than to use $x_1$ to predict the state at time $t_2$, and the larger $t_2 - t_1$ is, the less the accuracy of the prediction. Now, since observer 2 possesses more information about the state of the system — and the longer one waits to observe the state, the more one learns —, an expanding flow may be thought of as *creating information*.

In information theory, *information* is a quantity describing the degree of uncertainty of the state of the system. *Metric entropy*, introduced by A. N. Kolmogorov and Ya. G. Sinai (and therefore sometimes called the *Kolmogorov entropy* or the *K-S entropy*), is a number measuring the time rate of creation of information as a chaotic trajectory evolves. If the state of the system can be specified to within some tolerance $\epsilon > 0$, and $I(\epsilon,\tau)$ is the gain of information in a time interval $\tau$, then the metric entropy is defined as

$$H = \lim_{\epsilon \to 0} \lim_{\tau \to 0} \frac{I(\epsilon, \tau)}{\tau} . \tag{20}$$

In order to evaluate $H$, we divide the attractor $\Gamma$ of the system into $r$ disjoint elements $\Gamma_1, \Gamma_2, \ldots, \Gamma_r$ of size $\epsilon$, and the time into some intervals of

length $\tau$. We consider a segment of the trajectory which is known to be on the attractor and contains the observed phase points $x(\tau)$, $x(2\tau),\ldots,$ $x(k\tau)$. Let $p_i$ ($i = 1,2,\ldots,k$) be the probabilities of the chance that the points $x(i\tau)$ fall into the elements $\Gamma_i$. In this case

$$H = \lim_{k\to\infty} \lim_{\epsilon\to 0} \lim_{\tau\to 0} \frac{1}{k\tau} \sum_{i=1}^{n} p_i \ln \frac{1}{p_i}. \tag{21}$$

In well-behaved deterministic systems $H = 0$, in stochastic systems $H = \infty$, while in chaotic systems $H > 0$. It has been proven that the metric entropy is at most the sum of the positive Lyapunov exponents,

$$H \leq \Sigma\lambda_+ \tag{22}$$

(see, for example, *Ruelle*, 1989).

If we wish to express $H$ in binary units, we use $\log_2$ instead of ln in Eq. (21). In this case we can interpret $H$ as the gain of information in bits per unit time. Similarly, the sum of the positive Lyapunov exponents, also expressed in binary units, can be interpreted as measuring the rate in bits of information per unit time at which the uncertainty in the specification of initial data is magnified. Therefore, if the initial conditions are known accurately to $q$ bits, then after $q/\Sigma\lambda_+$ time units, on the average, the initial uncertainty will have contaminated the entire attractor.

### *2.3 Fractal dimensions*

As it was discussed above, in a chaotic dissipative system the flow does not contract a volume element in all directions, but stretches it in some. For a bounded system, however, the growth of $|\delta\mathbf{x}(t)|$ cannot be exponential forever; exponential growth must cease when $|\delta\mathbf{x}(t)|$ becomes of the order of the attractor size. In order to remain confined to this bounded domain of the phase space, the stretching volume element gets folded at the same time. As a result of the sequence of these stretching and folding processes, chaotic attractors possess a fine multisheeted structure. A closer study shows that the neighbourhood of any point of a chaotic, or strange attractor does not resemble any Euclidean space. Hence, strange attractors are not manifolds and do not have integer dimension. There are several ways to generalize the concept of dimension to this fractional case, and three are presented here.

Cover an attractor $\Gamma$ with volume elements each with diameter $\epsilon$. Let $N(\epsilon)$ be the number of volume elements needed to cover $\Gamma$. The *information dimension* $d_I$ is defined by

$$d_I = \lim_{\epsilon \to 0} \frac{\ln S(\epsilon)}{\ln (1/\epsilon)}, \tag{23}$$

where

$$S(\epsilon) = \sum_{i=1}^{N(\epsilon)} p_i \ln (1/p_i), \tag{24}$$

$p_i$ denoting here the relative frequency with which a typical trajectory enters the $i$th volume element of the covering (*Farmer et al.*, 1983). Thus information dimension weights a volume element according to how often a trajectory is found in it; volume elements that are visited infrequently have little influence on $d_I$. Comparing (24) with (21), we recognize $S(\epsilon)$ as entropy — the amount of information necessary to specify the state of the system to within an accuracy of $\epsilon$ if the state is known to be on the attractor. Eq. (23) may be rewritten as

$$S(\epsilon) = c(1/\epsilon)^{d_I} \tag{25}$$

for some constant $c$ and sufficiently small $\epsilon$. In words, the amount of information needed to specify the state increases inversely with the $d_I$th power of $\epsilon$.

Another probabilistic type of dimension is the *correlation dimension* $d_C$ defined by *Grassberger* and *Procaccia* (1983) as

$$d_C = \lim_{\epsilon \to 0} \left\{ \left[ \ln \sum_{i=1}^{N(\epsilon)} p_i^2 \right] \left[ 1 / \ln \epsilon \right] \right\}, \tag{26}$$

i.e. it also utilizes information about the time behaviour of the dynamical system. The correlation dimension is computationally very efficient to calculate even for attractors in high-dimensional phase spaces. It can be shown that $d_C \leq d_I$, and also that $n_+ \leq d_C$ for $n_+$ the number of positive Lyapunov exponents.

The *Lyapunov dimension* $d_L$ of an attractor is defined by *Kaplan* and *Yorke* (1979) in terms of the Lyapunov exponents $\lambda_i$ of a dynamical system as

$$d_L = j - \frac{\lambda_1 + \lambda_2 + \ldots + \lambda_j}{\lambda_{j+1}}, \tag{27}$$

where $j$ is the largest integer such that $\lambda_1 + \lambda_2 + \ldots + \lambda_j \geq 0$. Thus $d_L$ depends solely on the system dynamics. For a stable limit cycle, $0 = \lambda_1 > \lambda_2 \geq \lambda_3 \geq$

$\ldots \geq \lambda_n$, so $j = 1$ and $d_L = 1$ as expected. Likewise, for a two-torus, $d_L = 2$. In a three-dimensional chaotic dynamical system with $\lambda_+$, 0, $\lambda_-$,

$$d_L = 2 + \frac{\lambda_+}{|\lambda_-|}. \tag{28}$$

For an attractor, $\lambda_+ + \lambda_- < 0$, from which it follows that $2 < d_L < 3$.

As is obvious from the definition, Lyapunov dimension is somewhat different from the other two. In fact, it is not even clear that $d_L$ is actually a dimension. The exact relationship between $d_L$ and $d_I$ (and the other dimensions defined to the fractional case) is an active research topic.

Dimension is perhaps the most basic aspect of the attractor of a dynamical system. Generally speaking, the dimension provides a measure of the number of independent modes excited by the system, that is, it gives the minimum number of coupled nonlinear differential equations necessary to describe the system. On the other hand, the fractional part of the fractal dimension measures the 'strangeness' of a chaotic attractor.

### *3. Phases of error growth*

Let $\mathbf{x}(t)$ be the instantaneous state vector of a dissipative dynamical system. The system is run for a certain transient period of time until it reaches its attractor $\Gamma$. At this moment, which is regarded as the initial time 0, the state $\mathbf{x}(0)$ is slightly perturbed by an error vector $\delta\mathbf{x}(0)$. If the evolution of the initial state $\mathbf{x}(0)$ and the perturbed state $\mathbf{y}(0) = \mathbf{x}(0) + \delta\mathbf{x}(0)$ is followed simultaneously, the *instantaneous error* $E(t)$ at time $t$ is defined by $E(t) = \| \mathbf{y}(t) - \mathbf{x}(t) \|$, where $\| \ldots \|$ denotes the Euclidean norm. Because of the complexity of the dynamics of typical systems of interest, $E(t)$ fluctuates considerably both over time and over the phase space of the system. To relate the error dynamics in an intrinsic manner to the properties of the underlying system and to the structure of its attractor, the evaluation of $E(t)$ is repeated for initial conditions $\mathbf{x}(0)$ running all over the attractor $\Gamma$, and the *average error* over all these realizations,

$$< E(t) > = \frac{1}{2\mu(\Gamma)} \int_{\Gamma} d\mathbf{x}(0) \int_{\Gamma} \frac{\| \mathbf{y}(t) - \mathbf{x}(t) \|}{\| \mathbf{y}(0) - \mathbf{x}(0) \|} d\mathbf{y}(0) \tag{29}$$

is calculated, where $\mu(\Gamma)$ represents the measure of the phase-space region belonging to the attractor $\Gamma$.

The first systematic study of error growth was performed by *Lorenz* (1965). He noted that since the initially infinitesimal perturbations continue to grow

while they are still small, they must eventually cease to be small, whereupon the tangent linear equations (3) governing them will no longer hold. The errors have then left the *linear phase of growth* and entered the *nonlinear phase of growth*. During this second phase the growth rate must eventually subside, since ultimately the errors will become only as large as the difference between two randomly chosen states of the system. In other words, an initially infinitesimal isotropic error ball, which was evolving into an ellipsoid during the linear phase, would in the nonlinear phase ultimately take on the structure of the system's attractor.

This conclusion has been confirmed and further refined by later investigations, among others by the numerical experiments on error growth carried out recently by *Nicolis* and *Nicolis* (1991), and *Nicolis* (1992). They integrated dynamical systems of varying complexity, including the logistic map, the Bernoulli map and the Rössler flow (see *Ott*, 1993), as well as the minimal model of the general circulation of the atmosphere designed by Lorenz (see *Götz*, 1994). In all cases essentially the same behaviour could be observed, which may reasonably be summarized by the statement that error growth is an explosive phenomenon following a logistic-like curve (*Fig. 3*). In a wide class of chaotic systems, three different stages can be distinguished:

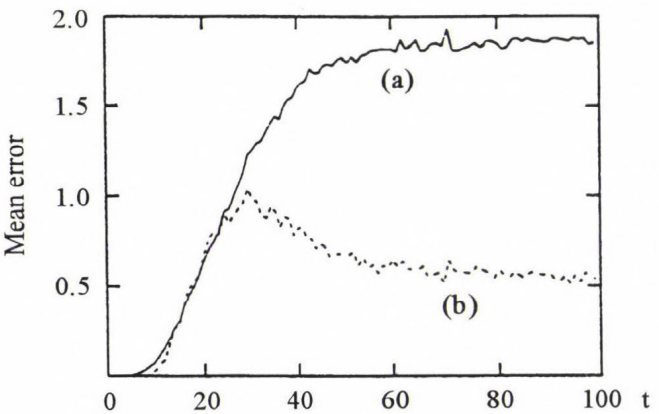


*Fig. 3.* (*a*) Time-dependence of the root-mean-square error over 1000 realizations for the Lorenz model of the general circulation. (*b*) Time-dependence of the variance of the error around the computed mean. The time unit is equal to five days. (After *Nicolis*, 1992)

(1) A short initial *exponential stage*, where errors remain small and are confined in the tangent space. This stage of error growth reflects local properties of the system and can be easily inferred from the very existence of a positive Lyapunov exponent.

(2) An *intermediate stage* around the inflexion point of the error versus time curve, where error growth displays an approximately linear dependence in time.

(3) A long *final stage* where, owing to the folding mechanism characteristic of chaotic attractors, the mean error reaches a saturation level $E_\infty$ of the order of the extension of the attractor, and remains constant thereafter. The intermediate stage is switched on at a time $t^*$ of the order of $t^* \approx \ln (1/|\delta \mathbf{x}|)$ when errors suddenly become large, they leave the tangent space and perform a diffusive motion on the attractor, while in the final stage errors essentially scan the structure of the attractor as a whole (*Fig. 4*). In this saturation stage, the variance of the cloud of perturbations $\sigma$ becomes equal to the climate variance of the system $\sigma_c$, which means that all deterministic predictability is lost. In practice, one must of course choose some fraction of $\sigma/\sigma_c = 1$ as defining the limit of dynamical predictability, e.g. 0.90 which is consistent with the standard errors of the climate and error variance estimates.

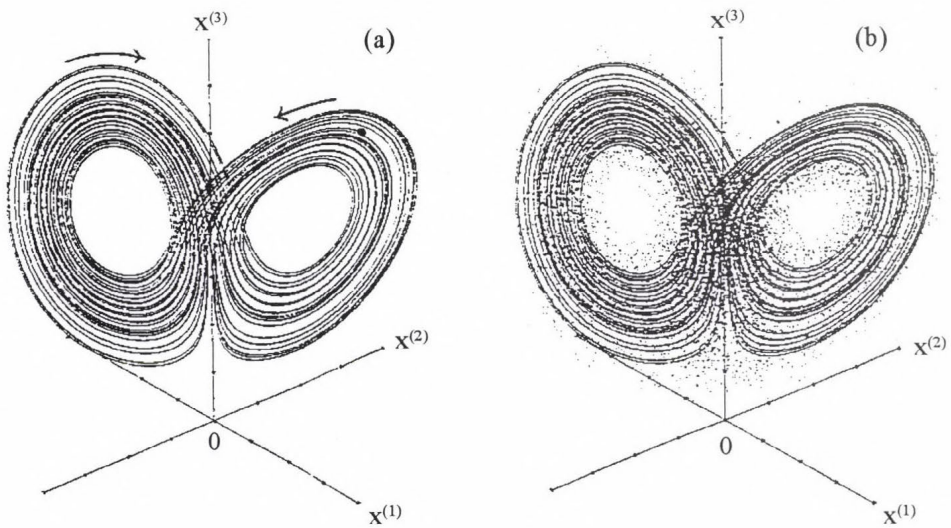


*Fig. 4.* The effect of divergence of initially nearby trajectories on the Lorenz attractor. The dot in (*a*) represents 10,000 initial conditions which are so close to each other that they are practically indistinguishable. If we allow each one of these states to evolve according to the governing equations of the system, in the saturation stage of error growth (*b*) the state of the system can be anywhere on the attractor. Arrows indicate the direction of the flow.

The first attempt to deduce the law of error growth from real atmospheric data is found in the work of *Lorenz* (1969). From a five-year record of Northern Hemisphere data, Lorenz selected all couples of states (called analogues) that are close enough to each other, that is, whose distance $\delta x$ can be considered small with respect to the average distance of two randomly

chosen states, and then looked at its temporal evolution. Lorenz proposed a quadratic law for the growth of average initial error $\delta x$ in the simple form of the logistic equation

$$\frac{d}{dt}\delta x = \lambda \delta x (1 - \delta x). \tag{30}$$

In this error equation, the linear term describes the initial exponential error growth, while the quadratic term enforces saturation at the variance of uncorrelated realizations. Lorenz based the hypothesis of a quadratic law on the argument that the principal nonlinearities governing the atmosphere are quadratic.

The solution of Eq. (30), with initial condition $\delta x(0)$, is

$$\delta x(t) = \frac{1}{1 + [1/\delta x\,(0) - 1]\exp(-\lambda t)}, \tag{31}$$

which asymptotically tends to the normalized mean distance 1 and shows an exponential growth for small errors with an $e$-folding time $t_e = 1/\lambda$. Eq. (30) is now often referred to as the *Lorenz's law of error growth*, and the coefficient of the linear term is just the quantity that was introduced some fifteen years later as the *first Lyapunov exponent* of the system (*Farmer et al.*, 1983).

While progress being made in nonlinear dynamics offers hope for a complete theory of predictability including both the intermediate stage and the final saturation stage, well-known methods suffice for understanding only the initial exponential stage by applying linearized small-error theory. Within this context, particular attention has been devoted in recent literature to the finding that the time evolution of initial errors can be actually more involved than outlined above. Within the framework of Oseledec's theory, the error perturbing the initial state of the system is bound to be *infinitesimal*, and therefore the error dynamics is confined in the tangent space, where it must be followed for an *infinitely* long period of time if it is to be related to intrinsic properties of the system. However, when confronted with the problem of predicting the evolution of a concrete physical system, the observer is led to follow the growth of a small but *finite* error over a *finite*, usually short period of time. As shown by *Nicolis* and *Nicolis* (1992), in this more realistic case the first transient phase of error growth is neither exponential, nor driven by the first Lyapunov exponent. They analysed the simple logistic map $x_{k+1} = rx_k (1 - x_k)$ with $r = 4$, i.e. in the region of fully developed chaos. In this system, the value of the Lyapunov exponent is $\lambda = \ln 2$. But for small finite initial errors the authors found that the effective growth rates are highly $k$-dependent,

starting at $k = 1$ with a value significantly larger than ln 2. This transient behaviour, that has been referred to as *superexponential*, entails that for short to intermediate times significant deviations from the Lyapunov-exponent driven exponential error amplification can be expected. This implies in no way a discrepancy with the Oseledec's theory: both the theory and the concept of Lyapunov exponent are perfectly valid, but are unable to account for error dynamics in the relevant regime of small finite errors and finite time.

Whereas transient error growth does not affect the dynamical predictability in the limit of infinitesimally small errors, it may have a dramatic impact on the predictability time for initial errors of a given finite size. As the initial errors cannot be reduced beyond certain limits, this problem may be of great practical importance for numerical weather prediction. Investigations carried out by *Lacarra* and *Talagrand* (1988), *Farrell* (1988, 1989, 1990), *Vukicevic* (1991), *Borges* and *Hartmann* (1992), and *Vannitsem* and *Nicolis* (1994) have revealed that the phenomenon of superexponential error growth is also related to the highly inhomogeneous dynamics on the generally multifractal attractor: during the initial transient phase, mean error amplification is controlled by high-energy perturbations that are not of normal-mode form and exhibit growth-rate values higher than the largest Lyapunov exponent. In order to investigate the impact of the transient error growth on average predictability measures, *Trevisan* (1993) considered the well-known three-dimensional convection model of *Lorenz* (1963). With Lorenz's original choice of parameter values, the spectrum of Lyapunov exponents for this nonlinear dynamical system is $\lambda_1 = 0.90$, $\lambda_2 = 0$, $\lambda_3 = -14.61$. *Fig. 5* shows the growth rate of linear errors as a function of time. During the transient, the ensemble-average error growth rate reaches values much larger than its asymptotic value. After the transient phase of the linear regime, the value of the growth rate stabilizes at about 0.90, in agreement with the value of $\lambda_1$ of the system.

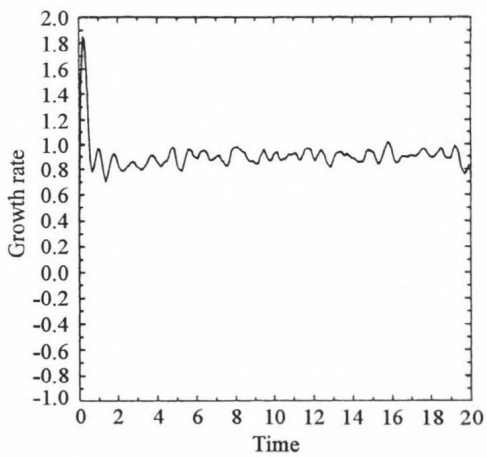


*Fig. 5.* Growth rate of linear errors as a function of time for the three-dimensional convection model of Lorenz. (After *Trevisan*, 1993)

For many years, it was widely believed that the energetically active synoptic-scale disturbances in the atmosphere arise primarily as exponentially growing normal-mode instabilities of the large-scale background flow. Therefore, the very existence of such a transient phase may be at first sight surprising, and can be explained as follows. For realistic basic-state flows, the error matrix $\boldsymbol{A}$ in Eq. (5) is not symmetric, and hence the eigenvectors of $\boldsymbol{A}$, corresponding to normal modes of dynamical instability, are not typically orthogonal to each other for the phase space of the linearized dynamics. This fact enables superposition of several normal modes to create non-modal perturbations for a limited time that grow very much faster than the most unstable normal-mode perturbation. In more mathematical terms, for non-self-adjoint $\boldsymbol{A}$ the largest singular value of $\boldsymbol{A}$ (from which the largest non-modal error growth rate is inferred) can be much larger than the largest eigenvalue of $\boldsymbol{A}$ (yielding the largest growth rate of the normal modes). Physically it can be argued from both observational and theoretical grounds that the variance associated with synoptic disturbances is connected with non-modal energy transfer from the background flow associated with stochastic forcing, which could arise, for example, from a nonlinear upscale energy cascade (*Farrell*, 1989). Consequently, predictability estimates for synoptic time scales made from the maximum normal-mode growth rate can be erroneously optimistic.

## *4. Predictability of weather and climate*

To facilitate study of the inherently infinite-dimensional partial differential equations governing the forced, dissipative, nonlinear atmospheric flow, spectral techniques are often employed, and the infinite set of transformed equations is truncated to a finite system of $n$ ordinary differential equations. The atmosphere is then represented as an $n$th-order autonomous dynamical system defined by the state equation (2), in which the components of the state vector $\mathbf{x}(t)$ are the spectral coefficients of a series of orthogonal functions, and the asymptotic solution sets (attractors) of Eq. (2) can be investigated in the more tractable setting of an $n$-dimensional phase space. The hope is that the essential behaviour characteristics of the atmosphere, for which an infinite number of degrees of freedom is available, can be adequately and faithfully modelled by a deterministic and reasonably low-dimensional system of appropriately chosen modes; for an overview of some of the results, see the article by *Götz* (1994).

In recent years, dynamical systems theory has provided a new quantitative perspective on the predictability of weather and climate processes. The interest in investigations that are using dynamical systems techniques is at least partially rooted in *Lorenz*'s (1965) observation that predictability is a function of the structure of the flow pattern. In addition, the interest in analysing predictability in phase space originates with the remarkable results of the Dynamical Systems

Collective at Santa Cruz, California (*Packard et al.*, 1980), *Ruelle* (1981) and *Takens* (1981) that it may be possible to deduce the unknown attractor of a physical system from a sufficiently long time series of just one state variable, without a knowledge of the evolution laws of the system. Once an attractor is properly reconstructed, the predictability measures discussed in Section 2 can be estimated (*Farmer* and *Sidorowich*, 1987; *Henderson* and *Wells*, 1988).

During the last few years, several researchers have tried to determine these quantitative measures for the atmosphere from model-generated output, as well as from observed data concerning both synoptic and climatic time scales. In this section, main results obtained for predictability limits are summarized.

### *4.1 Results based on model-generated data*

In 1963, Lorenz designed a three-dimensional nonlinear dissipative dynamical system in order to study the Rayleigh-Bénard convection. This low-order truncated spectral model not only correctly represents the initial transition from a conductive to a convective heat transport, but for suitable values of the control parameters it also exhibits the nonperiodic behaviour at more intense thermal forcing, that stimulated Lorenz to lay the foundation of the concept of deterministic chaos. As subsequently calculated by many authors, the correlation dimension of the system's attractor in its chaotic stage (at a slightly supercritical value of the Rayleigh number) is $d_C = 2.05$ with Lyapunov exponents $\lambda_1 = 0.9$, $\lambda_2 = 0$, $\lambda_3 = -14.6$. The average $e$-folding time of small initial errors is $t_e = 1/\lambda_1 = 1.1$ dimensionless time units. *Nese et al.* (1987) extended these calculations to higher-order truncations of the infinite set of ordinary differential equations from which the original Lorenz system is derived. For a seventh-order convection system, at values of the thermal forcing just above the initial transition to aperiodicity, they found $d_L = 4.06$, $H = \Sigma\lambda_+ = 1.43$, and $t_e = 0.7$ time units, while for an eleventh-order system, $d_L = 5.68$, $H = \Sigma\lambda_+ = 1.60$, and $t_e = 0.62$ time units.

Ten years ago, *Lorenz* (1984b) developed a third-order dynamical system as a minimal model of the general circulation of the atmosphere. This nonlinear, geostrophic baroclinic model possesses both Hadley- and Rossby-like solutions. In its chaotic regime, $d_L = 2.35$, $\lambda_1 = 0.18$, $\lambda_2 = 0$, $\lambda_3 = -0.52$, and $t_e = 1/\lambda_1 = 5.5$ time units (about 28 days). By real atmospheric standards, this error amplification is unreasonably small.

The appearance of persistent and recurrent regional weather types (*Grosswetterlagen*) has been long since known to synoptic meteorologists. However, low-order dynamical systems of *Lorenz* (1963, 1984b), *Charney* and *DeVore* (1979), and *Reinhold* and *Pierrehumbert* (1982) have offered the first theoretical explanation of the existence of such distinct flow regimes and the multiple time-scale evolution of the atmosphere in the presence of zonally inhomogeneous external forcing mechanism. There are two time scales

associated with these models. The first describes the evolution of the system around the weakly unstable fixed point at the centre of each wing of the Lorenz attractor (Fig. 4), while the second describes a typical residence time within one of the two wings which correspond, qualitatively, to blocked and zonal flow.

Most of the unpredictability of the Lorenz model arises from the divergence of nearby phase-space trajectories in the neighbourhood of the particularly unstable origin (representing the state of rest of the system), and the phase-spatial organization of local predictability is closely connected with the transitions between the flow regimes (*Nese*, 1989; *Mukougawa et al.*, 1991; *Palmer*, 1993). According to *Nese* (1989), in the convection model with Lorenz's original parameter choices, the local divergence rate $D(\mathbf{x})$ varies from -15 bits per nondimensional time unit (bpt) to 16 bpt (note that the largest Lyapunov exponent of the system is $\lambda_1$ = 0.9/time unit = 0.9/ln 2 bpt = 1.3 bpt; for synoptic considerations, unit nondimensional time in the model can be taken to correspond to about 10 days in the atmosphere). Adjacent trajectories converge most rapidly on average ($D$ = -5.6 bpt) as they approach the vicinity of the $x^{(3)}$-axis on tops of the attractor wings in Fig. 4. The divergence of initially nearby trajectories increases as they enter the 'splitting' region of the attractor; they diverge most rapidly on average ($D$ = 5.4 bpt) as they swing away from the vicinity of the unstable origin $\mathbf{x}$ = 0. The region near the origin is only moderately unpredictable in terms of average local divergence rates ($D$ = 3.8 bpt); nonetheless, when catastrophic separation of initially nearby trajectories occurs, the consequences in terms of forecast errors are extremely severe.

In order to quantify predictability in a more realistic dynamical system, *Legras* and *Ghil* (1985) have introduced a model that is governed by the equivalent-barotropic form of the equation for the conservation of potential vorticity on a sphere, with simplified topography, a forced mid-latitude zonal jet, and Ekman dissipation. The governing equation has been discretized through a truncated expansion in spherical harmonics, and a 25th-order autonomous dynamical system has been derived. The authors have found that as the intensity of the forcing (similar to a Rossby number) is increased (i.e., the validity of the geostrophic approximation is decreased), zonal-dominated sequences of the flow pattern become more and more frequent than blocking-dominated sequences, and the largest Lyapunov exponent of the system increases from $\lambda$ = 0.028 day$^{-1}$ to $\lambda$ = 0.095 day$^{-1}$. Thus, the average $e$-folding time of small errors decreases by a factor of 3 from $t_e$ = 36 days to $t_e$ = 11 days. The average of local divergence rates of nearby trajectories reveals a local mean $e$-folding time of errors $t_e$ = 14 days for flows dominated by blocked regimes, which decreases to $t_e$ = 9 days for zonal-dominated regimes. These results are in agreement with observations about the Rossby-number dependence of flow regimes and persistence: blocked regimes are associated with lower Rossby numbers; as the forcing is increased, zonal regimes tend to prevail, the evolution of the flow patterns in physical space is

observed to become more rapid and the irregularity of the flow in phase space increases, resulting in a less predictable evolution of the system.

In a recent study of predictability, *Nese* and *Dutton* (1993) used a two-layer moist general circulation model, in which the atmosphere is governed by baroclinic, quasi-geostrophic, mid-latitude, beta-plane dynamics, and the basic state variables are temperature, horizontal wind velocity and isobaric vertical velocity. They found that the correlation and Lyapunov dimensions of the system are $d_C = 5.6$ and $d_L = 6.9$, while the two largest Lyapunov exponents are $\lambda_1 = 0.062$ and $\lambda_2 = 0.004$ bits/day, and thus the average error doubling time is $t_d = 15.1$ days. The sum of the two largest local divergence rates is $D_1(\mathbf{x}(t)) + D_2(\mathbf{x}(t)) = 0.270$ bits/day, i.e., the instantaneous predictability measure is $t_d = 3.7$ days. Activating an oceanic circulation increases the average error doubling times of the atmosphere and the coupled atmosphere-ocean system by 10%, and the local error doubling times to $t_d = 4.4$ days.

Extended (10,000-year) simulations carried out by *Nese* and *Dutton* (1993) enabled them to draw some conclusions concerning the predictability of yearly averaged climatic states. The model exhibited variations in the annually averaged temperature $T$ within a range of about 3 K; changes in $T$ from year to year averaged 0.07 K in magnitude. These changes represent the *natural variability* of the model, since no conditions external to the atmosphere-ocean system were altered. Such warmings and coolings, if encountered in the actual atmosphere, are interpreted as *internal climatic variability*, traditionally regarded as an intrinsically unpredictable component of climatic change. Now, the sum of the positive Lyapunov exponents of the reconstructed attractors has proven to be $H = \Sigma\lambda_+ = 2.04$ bits per year for the inert ocean case, decreasing by 25% to $H = \Sigma\lambda_+ = 1.52$ bits per year when an active ocean circulation is included. These values correspond to average error doubling times of $t_d = 6$ months and $t_d = 8$ months, respectively, i.e. annually averaged climatic states are, indeed, highly unpredictable. On the other hand, one-third of the yearly averaged states have local error doubling times larger than 2 years, indicating that annual climatic states may, at times, be predictable, even without predictable variations in external forcing.

The results summarized above confirm that the oceans have a major influence on weather and climate processes, and profoundly affect the predictability of weather and climate as well. Including a slowly varying component such as an ocean in a weather or climate model enhances the memory of the system and thus improves predictability, especially of time-averaged climatic states. If a circulation is permitted to develop in the model ocean, then the additional inertia in the system further enhances predictability. It has been shown by many investigators that a coupled atmosphere-ocean system is more predictable than the atmosphere alone. *Tribbia* and *Baumhefner* (1988) suggest that fixed lower boundary conditions (such as prescribed sea-surface temperatures) may inhibit the natural equilibration of low-frequency motions

through interaction with the underlying surface, thus making interactive boundary-driven motions more predictable than fixed-boundary, externally forced motions.

### *4.2 Results based on observed data*

Following the pioneering work of *Nicolis* and *Nicolis* (1984), several authors have tried to reconstruct weather and climate attracting sets from various sampled time series of single state variables of the atmosphere in order to estimate different predictability measures on attractors, independent of any modelling.

*Predictability on synoptic time scales.* In an early study, *Fraedrich* (1987) selected daily values of surface pressure, observed at Berlin-Dahlem, for calculating weather predictability. He obtained $d_L = 6.8$–$7.1$ for the dimension of the reconstructed attractor, and $t_e = 12$–$17$ days for the $e$-folding predictability time scale. *Keppenne* and *Nicolis* (1989) carried out a dynamical systems analysis of atmospheric variability over the entire Western European region, using daily 500-mb geopotential time series from a number of stations. They calculated that two Lyapunov exponents are unmistakingly positive: $\lambda_1 = 0.023$ day$^{-1}$, $\lambda_2 = 0.014$ day$^{-1}$, i.e. one deals here with a hyper-chaotic attractor. The fact that the two positive $\lambda_i$ are comparable in magnitude suggests that the chaotic dynamics arises from the interference of two independent mechanisms of instability of comparable importance. The mean predictability time for the geopotential signal is $t_e = 27$ days, which is comparable but clearly larger than that inferred by *Fraedrich* (1987). Considering local rates of divergence, the authors found very strong variability. For values corresponding to low geopotential heights, the predictability is of the order of 30 days; it decreases to about 2 weeks for high geopotential values. These results are in agreement with the observed fact that in Europe, winter predictions are generally more satisfactory than summer ones. A less obvious and somewhat speculative conjecture is to associate a cyclonic weather pattern over Western Europe to the North-Atlantic blocking: the high persistence of the latter appears as the consequence of the high predictability of the low-geopotential part of the attractor.

In a similarly detailed analysis, *Zeng et al.* (1992) utilized the time series of daily surface temperature and pressure over several regions of the United States and the North-Atlantic Ocean for estimating the predictability of the atmosphere. They also found that at least two Lyapunov exponents are positive with comparative magnitude. The main results can be summarized as follows. For sea-surface temperatures in the Atlantic, metric entropy $H = \Sigma\lambda_+$ varies between 0.094 and 0.148 day$^{-1}$, therefore $t_e = 6.5$–$10.5$ days; for sea-surface pressure data in the Atlantic, $H$ varies between 0.101 and 0.142 day$^{-1}$, so that $t_e = 7$–$10$ days; for surface temperatures over the North-American continent,

$H$ = 0.186–0.276 day$^{-1}$, $t_e$ = 3.5–5.5 days; and for surface pressure over the North-American continent, $H$ = 0.402 day$^{-1}$, $t_e$ = 2.5 days; finally, a general conclusion: the predictability time in this region is larger in summer than in winter for all state variables. We can see that the time scales are smaller than those inferred by Keppenne and Nicolis. This discrepancy may be explained partly by the fact that $t_e$ depends on how the magnitude of initial errors is defined in the different calculations ($t_e$ is short for small initial errors and longer for larger initial errors), and partly by the fact that surface processes are less predictable than upper-air processes (see, e.g. *Yang*, 1991).

Among the specialized meteorological prediction problems, the forecasting of tropical cyclone tracks is generally identified as the one where obtaining a significant level of skill is very difficult. By applying nonlinear systems analysis methods to the evolution of tropical cyclone tracks in the Australian region, *Fraedrich* and *Leslie* (1989) found that the correlation dimensionality $d_C$ of the system is between 6 and 8, and that the *e*-folding error growth time scale is about 24 hours. In the case of mid-latitude cyclones in the North Pacific region, $t_e$ is between 4 and 7 days (*Fraedrich et al.*, 1990).

*Predictability on climatic time scales.* Much of our information on the evolution of the earth's climatic state during the past million years comes from the time series describing the isotope record of deep-sea cores. In their attractor reconstruction calculations, *Nicolis* and *Nicolis* (1984) used the oxygen isotope record obtained from the V-28-238 equatorial Pacific deep-sea core of N. J. Shackleton and N. D. Opdyke, and extended it over the past million years. They concluded in the existence of a low- (about three) dimensional attractor and a predictability time of about 30,000 years. Comparable results were obtained from the analysis by *Fraedrich* (1987), whose calculations were based on the oxygen isotope record gained from the *Meteor* 13519 deep-sea core in the eastern equatorial Atlantic, covering 775,000 years before present. Fraedrich's estimates have led to the existence of a climate attractor with the dimensionality $d_L$ = 4.4–4.8, and a climate predictability time scale $t_e$ = 10,000–15,000 years.

The occurrence of El Niño-Southern Oscillation (ENSO) episodes is highly irregular with time intervals between one and seven years. Therefore, it is not surprising that a similarity with a deterministic low-order chaotic system driven by the seasonal cycle has been suggested (see, e.g., *Göber et al.*, 1992; *Jin et al.*, 1994; *Tziperman et al.*, 1994). Nonlinear deterministic analysis of the annual time series of the ENSO carried out by *Fraedrich* (1988) has led to *e*-folding predictability time scales up to 1.5 years, indicating that at least a skillful nowcasting of ENSO may be possible. This conclusion is in agreement with numerical modelling results stating that ENSO is generally predictable one or two years ahead (*Brankovic et al.*, 1994).

Before closing this section, a short remark should be made concerning the reliability of the calculations aiming to reconstruct weather and climate

attractors. The existence of low-dimensional attractors that was found in most of these attempts is currently a highly debated subject; for more details of this problem, the reader is referred to the article by *Götz* (1994).

### *5. Ensemble prediction*

Since the notion of *predictability* is related to the rate of divergence of forecasts started from almost identical initial states, one potential method of estimating weather predictability is to construct an *ensemble* of possible initial states, each one being, *a priori*, equally likely. We can then integrate a deterministic numerical weather prediction model from each initial state, and produce an ensemble of forecasts for day 1, day 2 and so on. By studying the dispersion of the ensemble as the forecast proceeds, one can determine whether or not the uncertainties in the initial analyses were having a serious detrimental effect on forecast quality. Since each member of the ensemble is supposed to be equally likely, such a technique gives an essentially probabilistic forecast. In situations in which the ensemble of forecasts has a relative small dispersion, the predictability of the atmosphere is higher than average, and there is a high probability for some particular development. On the other hand, if initial uncertainties have amplified to such an extent that at a given forecast time the probabilities are spread more or less uniformly through a range of possible values then, for the particular state variable in question, the predictive skill has been lost (*Palmer et al.*, 1990).

The idea of ensemble forecasting was introduced in the context of numerical weather prediction by *Lorenz* (1965) and *Epstein* (1969). The technique was further developed by *Leith* (1974), who showed that if the uncertainties in the initial state are correctly specified, even with a relatively small ensemble size adequate accuracy can be obtained for the best mean of the forecast field. Their pioneering work has clearly revealed that the basic factors which determine the overall skill of an ensemble prediction are related to the questions of how large the size of an ensemble should be, and how best to generate the initial perturbations.

Probabilities based on very small initial sample sizes could be quite unrealistic. On the other hand, performing ensemble forecasts that have more than 100 members can be ruled out from practical considerations. Preliminary calculations suggest that there are about 50 important modes of instability for a realistic atmospheric flow. This number therefore represents approximately the ideal size of an ensemble, and may not be unreasonable from the point of view of development in computing technology as a result of the maturation of massively-parallel-processor architecture (*McPherson*, 1994).

Concerning the way in which the initial ensemble of states should be constructed, first we mention that, in some of the early attempts at producing

an ensemble prediction, the simple technique of adding to a given analysis a spatially uncorrelated random (Monte Carlo) perturbation at each model grid point was used. However, if we integrate such perturbed analyses forward in time, the dispersion of the ensemble may start to decrease, since arbitrary random perturbations will mainly project onto non-meteorological modes (inertia-gravity waves), which are generally decaying in the model. In such a situation, the eventual delayed dispersion of the ensemble leads to an overestimate of the predictability. In order to overcome this problem, we must ensure that all members of the manifold lie on the attractor of the system or, in other words, that they belong to the atmospheric *slow manifold* which consists of the set of all meteorological modes. But there is an even more important constraint to fix the initial ensemble, imposed by the dynamical instability properties of the basic flow. Uncertainties in the initial conditions are most important in regions where the flow is dynamically (baroclinically and/or barotropically) unstable. We therefore need to perturb the initial data in these regions, and with such a vertical and horizontal structure that will most readily excite the appropriate unstable normal modes. However, as we have seen, the normal-mode instabilities are by no means the fastest-growing (highest-energy) perturbations over periods of time relevant for short- and medium-range prediction: integrations up to 15 days have revealed that the growth rates of perturbations that are not of normal-mode form can be up to an order of magnitude larger than the most unstable normal-mode instability. These perturbations are often referred to as the *optimally growing errors*; their amplitudes can double in less than 12 hours and grow as much as 10-fold (energy as much as 100-fold) over 36 hours (*Molteni* and *Palmer*, 1993; *Buizza* and *Palmer*, 1994).

It is beyond the scope of this article to give details on the techniques that have recently been developed to calculate the optimally growing modes of instability of a given basic flow for the construction of the initial ensemble. In short, up to now two methods have been explicitly designed to generate efficient initial perturbations for ensemble forecasting. The 'optimal method', adopted at the European Centre for Medium-range Weather Forecasts (ECMWF), is based on a direct computation of the singular vectors of the tangent linear equations. The initial perturbations are constructed from 16 of the dominant singular vectors associated with the 36-hour *forecast* trajectory (*Palmer et al.*, 1992, 1994; *Buizza et al.*, 1993; *Mureau et al.*, 1993). The other method, developed at the U.S. National Meteorological Center (NMC), estimates the perturbations that *were* growing fastest during the 6-hour interval leading to the initial time $t_0$ by having introduced a small arbitrary perturbation on the control analysis at time $t_0$ – 6 hours. At time $t_0$, the difference between the control and perturbed forecasts is scaled back to the size of the original perturbation (a necessary step to keep the amplitude limited, since a *nonlinear* model is used), and this difference field is then added to the new analysis. As

the process is repeated forward in time, the scheme selects ('breeds') the modes that grow fastest during the cycle, and therefore this method has been denoted *breeding of the growing modes* (*Tracton* and *Kalnay*, 1993; *Toth* and *Kalnay*, 1993). For a sufficiently long period of time (about three days for the baroclinic atmosphere), these efficient perturbations asymptote to the local Lyapunov vectors in the phase space of the system. The conjecture of the method is that these are the well-organized perturbations present in the analysis cycle, leading to fast short-range forecast error growth.

A comparative verification of the two methods is not yet available. The ECMWF approach may be optimal in detecting the maximum range of possible forecast errors, while the NMC method may give a better estimate of the errors in the initial analysis.

Finally, for the sake of clarity, it might be important to emphasize that an uncertainty in the initial analysis is by no means the single source of forecast errors; incomplete model physics can, of course, also generate erroneous predictions. We know that the construction of a physically perfect model is probably quite as much an impossibility as the specification of perfect initial conditions. Yet, one of the most fundamental assumptions of the ensemble forecasting techniques is the *perfect-model hypothesis*. The reason of the necessity to introduce such an assumption is that if the numerical weather prediction model was not perfect, the control forecast and the model-generated unstable perturbations would characterize the stability conditions of the model itself, rather than those of the real atmosphere. Model-verification experiments have clearly revealed that, at least on global scales and on time scales of medium-range forecasts, the perfect-model hypothesis is satisfied in most of the synoptic situations in such a form that forecast errors arising from incomplete initial conditions are considerably larger than those resulting from model-physics deficiencies.

## *6. Concluding remarks*

The mathematical equations governing the dynamics of the atmospheric flow are nonlinear, and the observed structure of the atmosphere is characterized by horizontal and vertical gradients of air motion, temperature and humidity that permit hydrodynamical and thermodynamical instabilities to develop. Inevitable uncertainties in the initial state can grow due to the inherent instability of the flow and nonlinear interactions among motions of different space and time scales, placing a fundamental upper limit on the deterministic predictability of atmospheric behaviour.

Recent developments of the theory of dynamical systems have provided new techniques by which important information can be obtained concerning the extent of predictability of the system's evolution, independent of any modelling.

The predictability of a dynamical system is determined by the divergence of phase-space trajectory segments whose starting points are close. For chaotic systems, initially nearby trajectories diverge asymptotically at an exponential rate given by the positive Lyapunov exponents. These exponents are evaluated in the limit $t \rightarrow \infty$, and characterize many of the *global* (phase-space) properties of the associated attractor. However, the degree of divergence of *finite* segments of the trajectory depends strongly on the position of the starting points in the attractor set. Moreover, finite-time divergence rates need not be exponential, and can be much larger than those given by the Lyapunov exponents. Therefore, Lyapunov exponents are of limited use for studies of the *local* predictability properties of the system's attractor, that is of the dependence of perturbation growth on initial state. In recent years, much effort has been devoted to find the so-called *optimal excitation*, i.e. the perturbation that grows fastest on time scales of interest in numerical prediction.

The inherent deterministic forecasting limitation in nonlinear fluid-flow problems has motivated to try alternative approaches, like stochastic-dynamic modelling, statistical techniques and ensemble prediction. The ensemble technique reflects explicitly the recognition that the atmosphere is a chaotic system: here, a nonlinear deterministic numerical forecast is made several times from a set of perturbed initial states, each of which is, in principle, consistent with the available data. The choice of initial perturbation is guided by recent theoretical developments: a selection of the fastest-growing errors are used. By exciting the most energetically growing disturbances in the linear error-growth range, model-generated ensemble dispersion is then taken to be a measure of predictability.

The very existence of intrinsically imposed limits of predictability will undoubtedly have a lasting effect on the way to model or even monitor the environment. On the other hand, the average predictability times found for the evolution of the atmosphere on different time scales suggest that there is considerable room for improving forecast techniques for phenomena belonging to the relevant time scale.

**Acknowledgements**—The author is most grateful to the two anonymous reviewers, who made some particularly useful comments and suggestions to improve the original manuscript.

## *References*

*Abarbanel, H.D.I., Brown, R.* and *Kennel, M.B.*, 1991: Variations of Lyapunov exponents on a strange attractor. *J. Nonlinear Sci. 1*, 175-199.

*Benzi, R.* and *Carnevale, G.F.*, 1989: A possible measure of local predictability. *J. Atmos. Sci. 46*, 3595-3598.

*Bergeron, T.*, 1959: Methods in scientific weather analysis and forecasting. In *The Atmosphere and the Sea in Motion* (ed.: *B. Bolin*). The Rockefeller Institute Press and Oxford University Press, New York, pp. 440-474.

*Bjerknes, V.*, 1904: Das Problem der Wetter-

vorhersage, betrachtet vom Standpunkte der Mechanik und der Physik. *Meteor. Zeitschrift 21*, 1-7.

*Borges, M.D.* and *Hartmann, D.L.*, 1992: Barotropic instability and optimal perturbations of observed zonal flows. *J. Atmos. Sci. 49*, 335-354.

*Brankovic, C., Palmer, T.N.* and *Ferranti, L.*, 1994: Predictability of seasonal atmospheric variations. *J. Climate 7*, 217-237.

*Buizza, R.* and *Palmer, T.N.*, 1994: The singular vector structure of the general circulation. In *Research Activities in Atmospheric and Oceanic Modelling*, Report No. 19 (ed.: *G.J. Boer*). WMO/TD-No. 592, pp. 2.10-2.11.

*Buizza, R., Tribbia, J., Molteni, F.* and *Palmer, T.*, 1993: Computation of optimal unstable structures for a numerical weather prediction model. *Tellus 45A*, 388-407.

*Charney, J.G.*, 1951: Dynamic forecasting by numerical process. In *Compendium of Meteorology* (ed.: *T.F. Malone*). American Meteorological Society, Boston, pp. 470-482.

*Charney, J.G.* and *DeVore, J.G.*, 1979: Multiple flow equilibria in the atmosphere and blocking. *J. Atmos. Sci. 36*, 1205-1216.

*Charney, J.G., Fjörtoft, R.* and *von Neumann, J.*, 1950: Numerical integration of the barotropic vorticity equation. *Tellus 2*, 237-254.

*Epstein, E.S.*, 1969: Stochastic dynamic prediction. *Tellus 21*, 739-759.

*Farmer, J.D., Ott, E.* and *Yorke, J.A.*, 1983: The dimension of chaotic attractors. *Physica 7D*, 153-180.

*Farmer, J.D.* and *Sidorowich, J.J.*, 1987: Predicting chaotic time series. *Phys. Rev. Lett. 59*, 845-848.

*Farrell, B.*, 1988: Optimal excitation of neutral Rossby waves. *J. Atmos. Sci. 45*, 163-172.

*Farrell, B.F.*, 1989: Optimal excitation of baroclinic waves. *J. Atmos. Sci. 46*, 1193-1206.

*Farrell, B.F.*, 1990: Small error dynamics and the predictability of atmospheric flows. *J. Atmos. Sci. 47*, 2409-2416.

*Fraedrich, K.*, 1987: Estimating weather and climate predictability on attractors. *J. Atmos. Sci. 44*, 722-728.

*Fraedrich, K.*, 1988: El Niño/Southern Oscillation predictability. *Mon. Wea. Rev. 116*, 1001-1012.

*Fraedrich, K., Grotjahn, R.* and *Leslie, L.M.*, 1990: Estimates of cyclone track predictability. II: Fractal analysis of mid-latitude cyclones. *Quart. J. Roy. Meteor. Soc. 116*, 317-335.

*Fraedrich, K.* and *Leslie, L.M.*: 1989: Estimates of cyclone track predictability. I: Tropical cyclones in the Australian region. *Quart. J. Roy. Meteor. Soc. 115*, 79-92.

*Göber, M., Herzel, H.* and *Graf, H.-F.*, 1992: Dimension analysis of El Niño/Southern Oscillation time series. *Ann. Geophys. 10*, 729-734.

*Götz, G.*, 1994: Application of nonlinear dynamics in atmospheric sciences. Part II. Some examples. *Időjárás 98*, 65-86.

*Grassberger, P.* and *Procaccia, I.*, 1983: Characterization of strange attractors. *Phys. Rev. Lett. 50*, 346-349.

*Henderson, H.W.* and *Wells, R.*, 1988: Obtaining attractor dimensions from meteorological time series. In *Advances in Geophysics*, Vol. 30 (ed.: *B. Saltzman*). Academic Press, San Diego, pp. 205-237.

*Hirsch, M.W.* and *Smale, S.*, 1974: *Differential Equations, Dynamical Systems, and Linear Algebra.* Academic Press, New York, 358 pp.

*Jin, F.-F., Neelin, J.D.* and *Ghil, M.*, 1994: El Niño on the devil's staircase: Annual subharmonic steps to chaos. *Science 264*, 70-72.

*Kaplan, J.L.* and *Yorke, J.A.*, 1979: Chaotic behavior of multidimensional difference equations. In *Functional Differential Equations and the Approximation of Fixed Points* (eds.: *H.O. Peitgen* and *H.O. Walther*). Springer Lecture Notes in Mathematics, Vol. 730. Springer-Verlag, Berlin, pp. 228-237.

*Keppenne, C.L.* and *Nicolis, C.*, 1989: Global properties and local structure of the weather attractor over Western Europe. *J. Atmos. Sci. 46*, 2356-2370.

*Lacarra, J.-F.* and *Talagrand, O.*, 1988: Short-range evolution of small perturbations in a barotropic model. *Tellus 40A*, 81-95.

*Legras, B.* and *Ghil, M.*, 1985: Persistent

anomalies, blocking and variations in atmospheric predictability. *J. Atmos. Sci. 42*, 433-471.

*Leith, C.E.*, 1974: Theoretical skill of Monte Carlo forecasts. *Mon. Wea. Rev. 102*, 409-418.

*Lorenz, E.N.*, 1963: Deterministic nonperiodic flow. *J. Atmos. Sci. 20*, 130-141.

*Lorenz, E.N.*, 1965: A study of the predictability of a 28-variable atmospheric model. *Tellus 17*, 321-333.

*Lorenz, E.N.*, 1969: Atmospheric predictability as revealed by naturally occurring analogues. *J. Atmos. Sci. 26*, 636-646.

*Lorenz, E.N.*, 1984a: The local structure of a chaotic attractor in four dimensions. *Physica 13D*, 90-104.

*Lorenz, E.N.*, 1984b: Irregularity: A fundamental property of the atmosphere. *Tellus 36A*, 98-110.

*McPherson, R.D.*, 1994: Advances in operational numerical weather prediction: An outlook for the early twenty-first century. In *Lectures Presented at the Forty-fifth Session of the WMO Executive Council.* WMO-No. 805, pp. 7-12.

*Molteni, F.* and *Palmer, T.N.*, 1993: Predictability and finite-time instability of the northern winter circulation. *Quart. J. Roy. Meteor. Soc. 119*, 269-298.

*Mukougawa, H., Kimoto, M.* and *Yoden, S.*, 1991: A relationship between local error growth and quasi-stationary states: Case study in the Lorenz system. *J. Atmos. Sci. 48*, 1231-1237.

*Mureau, R., Molteni, F.* and *Palmer, T.N.*, 1993: Ensemble prediction using dynamically conditioned perturbations. *Quart. J. Roy. Meteor. Soc. 119*, 299-323.

*Nese, J.M.*, 1989: Quantifying local predictability in phase space. *Physica D 35*, 237-250.

*Nese, J.M.* and *Dutton, J.A.*, 1993: Quantifying predictability variations in a low-order ocean-atmosphere model: A dynamical systems approach. *J. Climate 6*, 185-204.

*Nese, J.M., Dutton, J.A.* and *Wells, R.*, 1987: Calculated attractor dimensions for low-order spectral models. *J. Atmos. Sci. 44*, 1950-1972.

*Nicolis, C.*, 1992: Probabilistic aspects of error growth in atmospheric dynamics. *Quart. J. Roy. Meteor. Soc. 118*, 553-568.

*Nicolis, C.* and *Nicolis, G.*, 1984: Is there a climatic attractor? *Nature 311*, 529-532.

*Nicolis, C.* and *Nicolis, G.*, 1991: Dynamics of error growth in unstable systems. *Phys. Rev. A43*, 5720-5723.

*Nicolis, C.* and *Nicolis, G.*, 1993: Finite time behavior of small errors in deterministic chaos and Lyapunov exponents. *Int. J. Bifurcation and Chaos 3*, 1339-1342.

*Oseledec, V.I.*, 1968: A multiplicative ergodic theorem. Lyapunov characteristic numbers for dynamical systems. *Trans. Moscow Math. Soc. 19*, 197-231.

*Ott, E.*, 1993: *Chaos in Dynamical Systems.* Cambridge University Press, Cambridge, 385 pp.

*Packard, N.H., Crutchfield, J.P., Farmer, J.D.* and *Shaw, R.S.*, 1980: Geometry from a time series. *Phys. Rev. Lett. 45*, 712-716.

*Palmer, T.N.*, 1993: Extended-range atmospheric prediction and the Lorenz model. *Bull. Amer. Meteor. Soc. 74*, 49-65.

*Palmer, T.N., Buizza, R., Molteni, F.* and *Mureau, R.*, 1994: The ECMWF ensemble prediction system. In *Research Activities in Atmospheric and Oceanic Modelling*, Report No. 19 (ed.: *G.J. Boer*). WMO/TD-No. 592, pp. 6.17-6.18.

*Palmer, T., Molteni, F., Mureau, R., Buizza, R., Chapelet, P.* and *Tribbia, J.*, 1992: *Ensemble Prediction.* ECMWF Research Department Tech. Memo. No. 188.

*Palmer, T.N., Mureau, R.* and *Molteni, F.*, 1990: The Monte Carlo forecast. *Weather 45*, 198-207.

*Parker, T.S.* and *Chua, L.O.*, 1987: Chaos: A tutorial for engineers. *Proc. IEEE 75*, 982-1008.

*Reinhold, B.B.* and *Pierrehumbert, R.T.*, 1982: Dynamics of weather regimes: Quasi stationary waves and blocking. *Mon. Wea. Rev. 110*, 1105-1145.

*Richardson, L.F.*, 1922: *Weather Prediction by Numerical Process.* Cambridge University Press, Cambridge, 236 pp.

*Ruelle, D.*, 1981: Chemical kinetics and differentiable dynamical systems. In *Nonlinear Phenomena in Chemical Dynamics*

(eds.: *A. Pacault* and *C. Vidal*). Springer-Verlag, Berlin, pp. 30-37.

*Ruelle, D.*, 1989: *Chaotic Evolution and Strange Attractors*. Cambridge University Press, New York.

*Shukla, J.*, 1985: Predictability. In *Advances in Geophysics*, Vol. 28B: Weather Dynamics (ed.: *S. Manabe*). Academic Press, Orlando, pp. 87-122.

*Takens, F.*, 1981: Detecting strange attractors in turbulence. In *Dynamical Systems and Turbulence* (eds.: *D.A. Rand* and *L.-S. Young*). Warwick 1980 Lecture Notes in Mathematics, Vol. 898. Springer-Verlag, Berlin, pp. 366-381.

*Thompson, P.D.*, 1957: Uncertainty of initial state as a factor in the predictability of large scale atmospheric flow patterns. *Tellus 9*, 275-295.

*Toth, Z.* and *Kalnay, E.*, 1993: Ensemble forecasting at NMC: The generation of perturbations. *Bull. Amer. Meteor. Soc. 74*, 2317-2330.

*Tracton, M.S.* and *Kalnay, E.*, 1993: Operational ensemble prediction at the National Meteorological Center: Practical aspects. *Wea. Forecasting 8*, 379-398.

*Trevisan, A.*, 1993: Impact of transient error growth on global average predictability measures. *J. Atmos. Sci. 50*, 1016-1028.

*Tribbia, J.J.* and *Baumhefner, D.P.*, 1988: Estimates of the predictability of low-frequency variability with a spectral general circulation model. *J. Atmos. Sci. 45*, 2306-2317.

*Tziperman, E., Stone, L., Cane, M.A.* and *Jarosh, H.*, 1994: El Niño chaos: Overlapping of resonances between the seasonal cycle and the Pacific ocean-atmosphere oscillator. *Science 264*, 72-74.

*Vannitsem, S.* and *Nicolis, C.*, 1994: Predictability experiments on a simplified thermal convection model: The role of spatial scales. *J. Geophys. Res. 99*, 10,377-10,385.

*Vukicevic, T.*, 1991: Nonlinear and linear evolution of initial forecast errors. *Mon. Wea. Rev. 119*, 1602-1611.

*Yang, P.*, 1991: On the chaotic behavior and predictability of the real atmosphere. *Adv. Atmos. Sci. 8*, 407-420.

*Zeng, X.*, 1992: *Chaos Theory and Its Application in the Atmosphere*. Department of Atmospheric Science, Colorado State University, Atmospheric Science Paper No. 504.

*Zeng, X., Pielke, R.A.* and *Eykholt, R.*, 1992: Estimating the fractal dimension and the predictability of the atmosphere. *J. Atmos. Sci. 49*, 649-659.

# IDŐJÁRÁS

*Quarterly Journal of the Hungarian Meteorological Service*
*Vol. 99, No. 1, January–March 1995*


# Problems in lysimeter use for determining the water demand of sugar beet


**Angéla Anda**

*Pannon Agricultural University,*
*P.O. Box 71, H-8361 Keszthely, Hungary*



*(Manuscript received 5 January 1995; in final form 15 March 1995)*



**Abstract**—Investigation on evapotranspiration and changes in plant features as assimilatory surface, stomatal resistance, soil temperature and plant production of three different sugar beet varieties grown at non-limited water supply in Thornthwaite type compensation evapotranspirometers (or lysimeters) were carried out at Keszthely, Hungary, during the 1992 growing season. (The surface area of soil containers of the evapotranspirometers was 4 $m^2$, the depth of them was 1 m.) Already in the early stage of plant development it became evident, that the water supply and the ratio of soil moisture and soil air in the containers of lysimeters were not advantageous for sugar beet growing (size and color of leaves). The assimilatory surface of plants grown in lysimeters decreased significantly, and caused differences also in parameters of microclimate (soil and air temperatures, relative humidity of air) and other plant characteristics as compared to the control treatment. The LAI in the irrigated treatments decreased considerably, and caused increase in soil surface temperatures. The higher the soil temperature, the larger the stomatal resistance was experienced in watered canopies. These symptoms were completely contrary to our expectations. The direction of change in plant characteristics of irrigated treatments has a negative influence on plant sugar production, where the yield depressions were between 3.2 and 40.9% depending on crop variety.

There was significant difference in measured plant and microclimatic parameters of the three cultivars as well. In spite of higher soil moisture of lysimeters there was a strong decrease in sugar production of *Gála* and *Kawemaya* varieties. Either studied crop parameters or production of watered *Éva* cultivar has changed on the least extent as compared to the control ones, that means different sensitivity of the three sugar beet varieties for altered environmental (soil water) conditions. The change in soil air-water ratio resulted from continuous water supply in the lysimeter soil had negative effect on production of two beet cultivars. To determine the sugar beet water demand correctly, other water supply methods of containers or deeper lysimeter tanks would be necessary.



*Key-words:* sugar beet, evapotranspiration, yield and quality, soil temperature, stomatal resistance, LAI, sugar beet varieties.

## *1. Introduction*

The main characteristic of the climate of Hungary is the tendency for dryness and frequent drought. To cope with shortage of rainfall irrigation is needed. To plan irrigation correctly, both plant water demand and precipitation should be followed during the whole vegetative period. To measure the amount of rainfall is out of problem, but the exact determination of evapotranspiration of plant stands involves both technical and theoretical difficulties. One of the instruments fulfilling the purpose of following plant water losses is the lysimeter or evapotranspirometer. In the frame of Hungarian Meteorological Service investigations on lysimeter use for plant water demand measurements has been carried out from the early 60-es (*Antal* 1966a, 1966b; *Antal* and *Posza*, 1967). Further on these investigations *Antal* (1968a, 1968b) developed his method to estimate the evapotranspiration of different plant stands.

In the first decade of investigations meteorological and agricultural researchers have studied variation in water loss of arable crops (*Antal,* 1966a, 1972; *Antal* and *Posza*, 1967, 1970; *Petrasovits,* 1970; *Antal* and *Endrődi*, 1972; *Erdős,* 1966; *Szlovák,* 1979; *Fekete* and *Szilágyi*, 1979; *Endrődi,* 1979; *Kádár* and *Szilágyi*, 1980), then the evapotranspiration investigations were concentrated to vegetable plants, fruit trees and vineyard (*Kozma* and *Füri*, 1974; *Stollár* and *Gergely*, 1978; *Novák* and *Szilágyi*, 1980; *Posza,* 1980; *Cselőtei,* 1991; *et al.*). From second decade of experiments the evapotranspiration studies were applied to explain other environmental (agricultural) phenomena such as for example water balance changes resulting from using different amounts of artificial fertilizers (*Antal et al.*, 1975; *Tóth*, 1978; *Ruzsányi,* 1975, 1981), plant densities (*Walkowszki,* 1978), or effect of soil water table (*Szalóki,* 1971; *Posza,* 1978).

As there were merely publications in Hungary on changes in microclimatic and some of the plant characteristics of sugar beet when growing them in lysimeters, the goal of our experiment was to measure a few water balance components together with alteration of microclimate, and plant elements of three different sugar beet varieties grown at non-limited water supply in lysimeter containers. Parallel evapotranspiration investigations other plant features as leaf area, stomatal resistance and production of sugar beet were also studied. Detailed investigations on determining sugar beet water consumption by using lysimeter measurements has been carried out under Hungarian climatic conditions earlier by *Antal* and *Posza* (1970), *Endrődi* (1973, 1974), and *Ruzsányi* (1990).

## *2. Material and methods*

Investigations were carried out on sugar beet grown in Thornthwaite type compensation evapotranspirometers at Keszthely Agrometeorological Research Station, Hungary, during the 1992 growing season. Three sugar beet varieties

(*Kawemaya* — widely used in Europe, bred in Germany, *Gála* and *Éva* — two Hungarian varieties) were sown into lysimeter-soil containers (tanks) filled with Ramann type brown forest soil. The soil surface area of tanks 4 $m^2$ and the depth of them 1 m. Plant density was among 10 to 12 per $m^2$. Daily sum of evapotranspiration was calculated by following the water balance components of plant stands by using the original method of *Antal* (1968b). The comparison of evapotranspiration of different beet varieties was made with the help of calculated pentad means of water losses and by using transpiration intensity per unit leaf area.

Simultaneously with lysimeter measurements, the above mentioned three sugar beet cultivars were grown at natural rainfall only (control). Both the sizes of control plots and plant density were the same as used in lysimeter tanks. Altogether we had 6 treatments: 3 beet cultivars grown in lysimeters and the same 3 under natural rainfall only. The number of replications was 4.

Leaf area of sugar beet crops was measured on 5 plants in each of the treatments by LI-3000 type portable planimeter in every two weeks. The size of assimilatory surface was explained with leaf-area-index (LAI).

Stomatal resistance was determined by LI-60 type diffusive porometer on 3 to 5 sunlit upper leaves on 5 days with completely clear sky conditions hourly between 8 to 17 h with the aim of getting comparable results the age of leaf, place of measurement on blades (upper third of leaf from the stem) and orientations of sample leaves were more or less the same.

Because of well-known heterogeneity of soil structure and temperature, instead of point measurements by using traditional mercury thermometers, a new method was introduced to determine the actual plot-soil surface temperature (*Anda,* 1993). A Raynger II.RTL type infrared thermometer was applied to determine soil surface temperature on the same 5 days of the growing season when stomatal resistance was also measured. Diurnal variation of soil temperature was characterized by representing the hourly values each sample day.

In the end of the vegetation period sugar yield per unit soil area was determined by measuring both the root yield and sugar content of roots.

As there was no significant difference in plant- and other characteristics between irrigated and non-irrigated treatments of *Éva* cultivar, mainly the results of the other two varieties will be represented. When it is necessary, measurements for *Éva* will also be shown and analyzed.

## *3. Results and discussion*

### *3.1 Assimilatory surface*

The change in architecture of plant stand has of primary importance in plant studies, because they influence distribution of other crop- and microclimatic parameters determining plant production. In our study architecture of plant stands was therefore characterized by leaf-area-index.

The green leaf size among both three cultivars and irrigated and control treatments differed significantly during the 1992 growing season, mainly after the canopy closure. In lysimeters *Éva* had by 27.6 percent higher LAI than that of the assimilatory surfaces of *Kawemaya*, the variety of the smallest leaf area. The LAI values of *Gála* were between the other two cultivars. In control canopies the order of assimilatory surface size of different sugar beet varieties was completely different: the *Kawemaya* had the largest LAI, and the decreases in annual LAI mean of *Gála* and *Éva* was 11.7 and 33.8 percent respectively, as compared to the LAI values of *Kawemaya*.

In contrary with our expectations, the continuous high soil moisture content in the lysimeter tanks resulted in a decrease of yearly LAI averages in *Kawemaya* and *Gála* by 65 and 34 percent respectively, comparing to the LAI of non-irrigated control varieties *(Fig. 1)*. The time of developing maximum green leaf area appeared two weeks earlier in growing tanks of lysimeter considering *Kawemaya* and *Gála* varieties. As it was mentioned in Introduction chapter, either the LAI or its maximum value has not changed significantly in variety *Éva* as a result of increased soil moisture content.

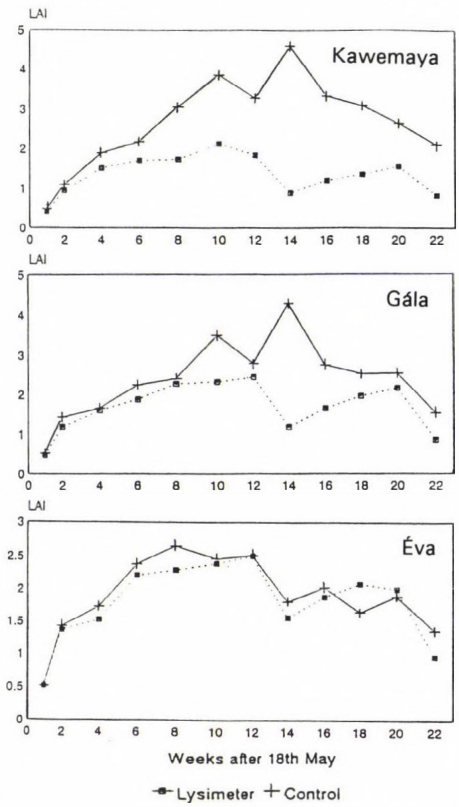


*Fig. 1.* Leaf area index of different sugar beet varieties.

The sensitivity of three different beet cultivars for increased soil moisture content was not the same. Variety *Éva* of least green leaf size and production showed the fewest sensitivities for continuous high soil water level (0.9 m from the soil surface in 1 m deep lysimeter tanks). The other two sugar beet varieties, the *Kawemaya* and *Gála* of increased assimilatory surface and yield were hypersensitive to changed soil water and air ratio. Unhealthy colored yellow plants in lysimeter tanks with decreased assimilatory leaf surface showed that there is a water supply problem when the sugar beet grows in relatively shallow evapotranspirometer tanks. Probably there was an out of air shortage problem in the root zone of the compensation lysimeter during the dry and warm growing season of 1992. The similar symptom was experienced by *Endrődi* (1973, 1974).

### *3.2 Plant water balance components*

Growing season of 1992 was drier and warmer than in usual, especially in the second half of investigation period (from the end of July to the end of August), when the daily sum of potential evapotranspiration frequently reached the 7–8 mm, and never decreased below 4 mm. Until the end of August the daily mean of air temperature values often approached to 25°C measured at the Agrometeorological Research Station of Keszthely. Sum of precipitation during July and August was altogether 58 mm only. The ratio of precipitation and potential evapotranspiration was 68.3 percent for the whole growing season of 1992, meaning a dry and warm vegetation period during 1992.

There were no significant differences in the summarized evapotranspiration sums among the three sugar beet varieties grown in evapotranspirometers. Like a tendency, the water loss of *Éva* increased by 3.5 percent, comparing to the evapotranspiration of the other two varieties. Oppositely to summarized water consumption, the transpiration intensity in the different treatments has changed significantly *(Fig. 2)*. The variety of *Kawemaya* had the highest (evapo)transpiration intensity of all. Decrease in annual average of transpiration rate of the other two cultivars were 17.4 and 24.3 percent in *Gála* and *Éva* plant stands, respectively. The cause of increased water loss of *Kawemaya* might have been associated with change in microclimatic conditions resulting from altered assimilatory surface of irrigated plants. The soil surface temperature measurements seemed to justify this assumption during 1992.

### *3.3 Soil surface temperatures*

The likely reason of increased transpiration intensity of *Kawemaya* might have been associated with decreased size of shadowing leaf area causing higher soil heat accumulation. The higher the soil temperature, the larger the transpiration was in irrigated treatments. In this experiment the change in soil surface

temperature resulting from alteration in shadowing leaf area was much higher when comparing the irrigated and non-irrigated treatments *(Fig. 3a)*. Difference in annual average of the soil temperature between watered and control plants was 2.8 and 2.4°C in *Kawemaya* and *Gála* canopies, respectively. The time of appearing of highest temperature changes occurred in the afternoon hours *(Fig. 4)*, when the soil temperature of lysimeters was sometimes 3 to 5°C warmer, than that of the controls. Independently, on both beet cultivars and assimilatory surface size in the morning hours an opposite tendency occurred, and the soil surface temperature in the control treatments was about 0.5 to 1°C warmer than the temperature of lysimeters in the top soil. The likely reason might have been associated with water-filling up of upper soil layer of evapotranspirometer tanks, during the night, when there was enough time for capillarity to reach the top soil also. This water evaporates easily in the early morning and cools the soil surface temperature in the evapotranspirometer tanks. Later, with higher insolation and soil warming, there is not enough time to filling up with water, and the subsoil irrigation water originating from the bottom of lysimeter tanks can not compensate the increasing rate of evaporation. After 10–11 h, the size of assimilatory surface plays leading role in determination of actual soil surface temperatures.

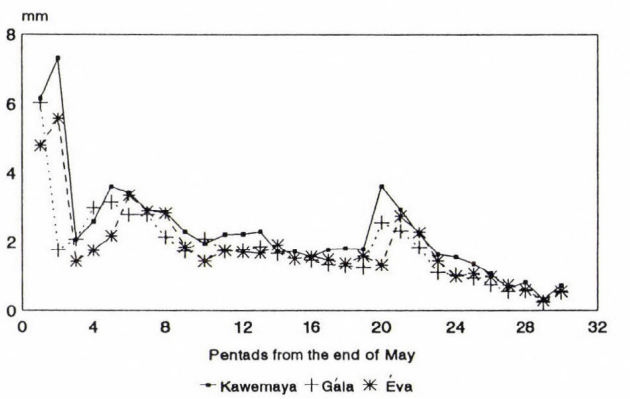


*Fig. 2.* Intensity of evapotranspiration in sugar beet in Keszthely, 1992.

The change in soil heat accumulation of watered canopies caused other differences in parameters of microclimate. The higher the soil temperature in lysimeters, the warmer and drier the air was at about 1 m above the plant stand. Size of change resulting from altered plant growing conditions depended on time of day. At low sun radiation there was no difference in measured micrometeorological elements. At high radiation level the air about 1 m above irrigated crops was 1.5 to 2.5°C warmer and 10 to 15 percent richer in relative

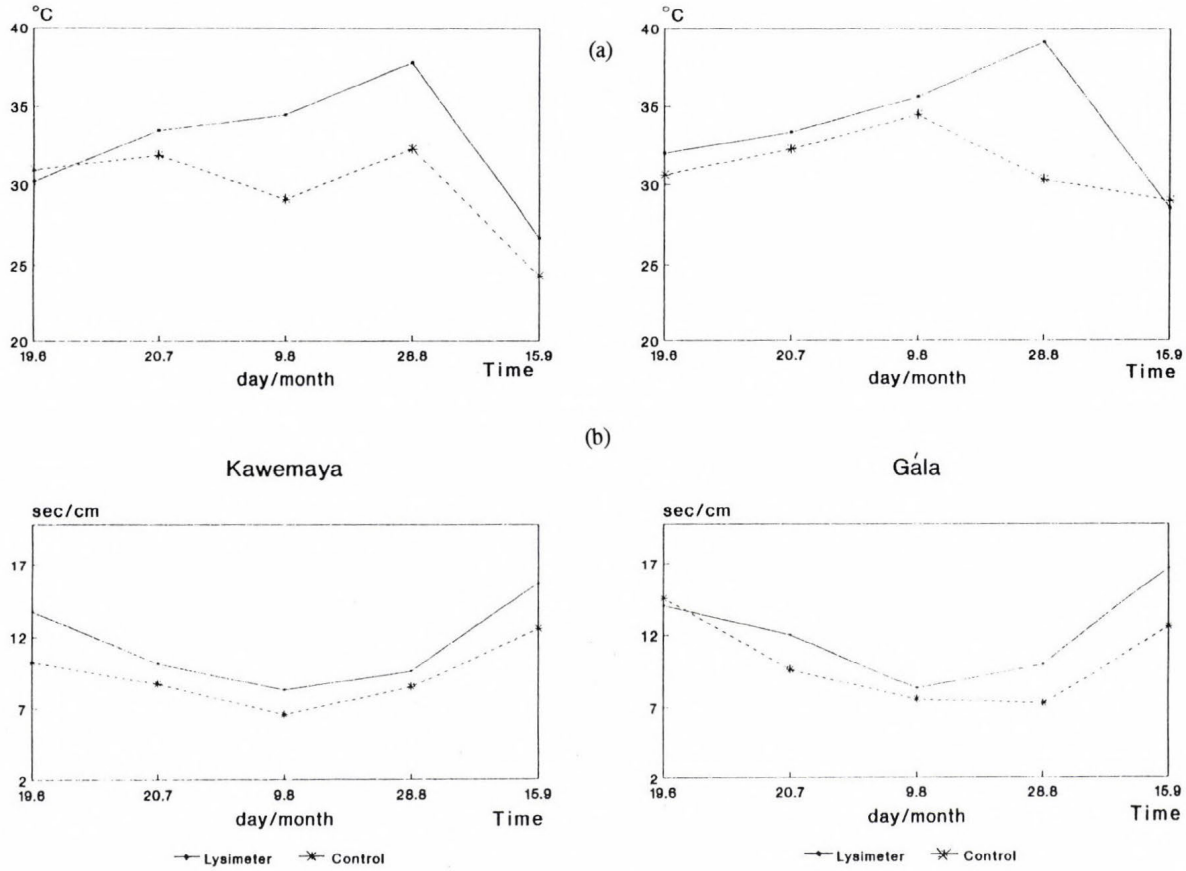


*Fig. 3.* Annual changes in soil surface temperature (*a*) and stomatal resistance (*b*).

humidity content than the air of control plant stands. Because of LAI depression and soil temperature increase at watered canopies, in contrary with expectations, the irrigated canopies had warmer and drier microclimate.

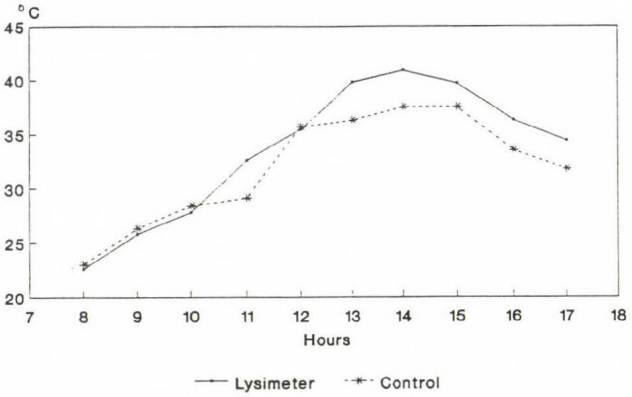


*Fig. 4.* Diurnal variation of soil temperature in *Kawemaya* on 19th July, 1992.

### *3.4 Stomatal resistance*

Alterations in stomatal resistance of different varieties were in accordance with soil temperature and microclimatic changes. Analyzing the relationship between the soil surface temperature and the stomatal resistance a linear relationship was determined. The increase in 1 °C of soil temperature caused a 0.7 sec/cm decrease in stomatal resistance during the measuring period of 1992 independently of water supply. In *Kawemaya's* canopy both the soil and air temperature values were the highest and the average stomatal resistances were the lowest of all. The low stomatal resistance means of largest pore-apertures caused the highest transpiration intensity of *Kawemaya* canopy. The increase in annual mean resistance of *Gála* and *Éva* was 5.9 and 29.6 percent, respectively.

Stomatal resistance determined in control canopies showed strong decrease comparing to the resistance of plants grown in lysimeter-container *(Fig. 3b).* The measures of change in annual means were 20.9 and 16.9 percent in *Kawemaya* and *Gála,* respectively. There was only one exception, the variety *Éva*, where the subsoil irrigation did not cause significant difference in diffusion resistances. Like a tendency, the largest changes in resistance of plants grown in lysimeter appeared in the afternoon hours *(Fig. 5).* As there was no difference in diurnal course of resistances between the varieties, the results determined in *Kawemaya* canopy will be shown only. The influence of irrigation on stomatal resistance occurred mainly in the afternoon hours. The irrigated sugar beet crops' behavior was completely opposite to the measured

resistances of watered plants by *Lawlor* and *Milford* (1975) and *Huzulak* and *Matejka* (1992). It is important to mention that these investigators used surface irrigation method and not lysimeters with subsurface irrigation. Increase in resistance of lysimeter's plants showed other than water shortage problem when sugar beet is grown in 1 m deep lysimeter tanks. At first, decreased and yellow colored leaves made us think shortage of minerals, mainly lack of nitrogen. Partial leaf-analysis refuted this assumption. The real cause might have been shortage of air in soil of lysimeter-containers resulted from continuous high soil water level. It seems, that the sugar beet is more sensitive to proper soil air-water ratio than that of the other earlier grown plants in lysimeter.

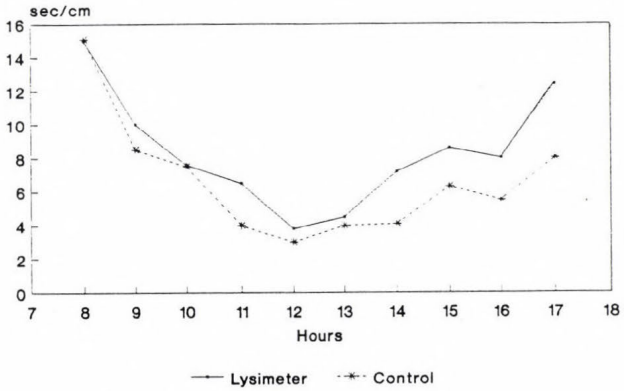


*Fig. 5.* Diurnal course of stomatal resistance in *Kawemaya* on 9th August 1992.

### *3.5 Plant production*

Similarly to summarized evapotranspiration, there was no significant difference in sugar production per unit soil area of three beet varieties at non-limited water supply. The excess water equalized the productivity of different cultivars, while unfavorable air-water conditions of lysimeter soil caused in 45.9 and 33.3 percent sugar yield decrease of *Kawemaya* and *Gála*'s treatment, respectively *(Fig. 6)*. The variety *Éva* produced the least and not significant yield depression to changed soil air-water ratio of all (3.2 percent).

The higher the produced sugar yield, the better the sugar beet variety was, when growing them without irrigation. In our experiment the above mentioned fact may be substituted with the following: the better the sugar beet cultivar at limited water supply, the more sensitive is, when growing them in shallow lysimeter's container. At control, the *Kawemaya* was the best yielded variety of all. The yield depressions of *Gála* and *Éva* were 5.9 and 40.3 percent, as compared to the production of *Kawemaya* at natural rainfall. In our one year

experiment, the variety of high-production property was more sensitive to proper environmental and growing conditions, among others for optimal air-water ratio in the soil than that of the other beet canopies. The best yielded variety, the *Kawemaya* may be grown on well aerated 'easy' soil types mainly. Change in sugar production of *Éva* (variety with least productivity at control condition) was negligible when changing the proper environmental conditions for growing sugar beet. It is the task of plant growers to reconcile the environmental condition of their growing area with the necessity of different sugar beet varieties of changed sensitivity.

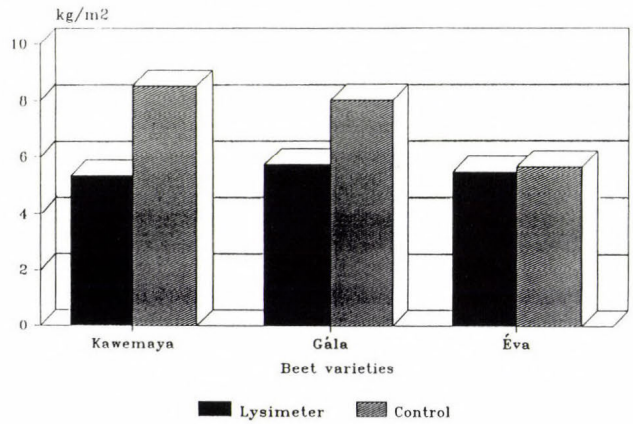


*Fig. 6.* Sugar production of different varieties.

## *References*


*Anda, A.*, 1993: Surface temperature as an important parameter of plant stand. *Időjárás 97*, 259-267.

*Antal, E.*, 1966a: Measurement of maximum water use in maize and alfalfa canopies (in Hungarian). *Beszámolók* 1964 II. Orsz. Meteor. Int., Budapest, 60-65.

*Antal, E.*, 1966b: Potential evapotranspiration of some agricultural crops (in Hungarian). *Öntözéses Gazdálkodás*, *4*, 69-86.

*Antal, E.*, 1968a: New method for determining of potential evapotranspiration (in Hungarian). *Beszámolók 1967*. Orsz. Meteorológiai Int., Budapest, 452-460.

*Antal, E.*, 1968b: *Forecast of Irrigation by Using Meteorological Elements*. Ph. D. Thesis, Budapest.

*Antal, E.*, 1972: Is plant growth determined by internal water balance and turgor in the cells or by external factors? *Acta Agronomica, Hungarian Acad. Sci. 21*, 458-468.

*Antal, E.* and *Posza, I.*, 1967: Characteristics of evapotranspiration in maize stand. *Beszámolók* 1966. Orsz. Meteorológiai Int., 499-509.

*Antal, E.* and *Posza, I.*, 1970: Biological crop constants of differenr plants and their change during the growing season (in Hungarian). *Beszámolók* 1968. Orsz. Meteorológiai Int., 452-460.

*Antal, E.* and *Endrődi, G.*, 1972: Water demand and irrigation water demand of potato (in Hungarian). *Időjárás 76*, 223-233.

*Antal, E., Posza, I.* and *Tóth, E.*, 1975: Influence of weather and climate on use of artifical fertilizer (in Hungarian). *Időjárás 79*, 95-104.

*Cselőtei, L.*, 1991: Basis of irrigation in growing of vegetables (in Hungarian). *GATE Hiv. Kiadv.*, Gödöllő, pp. 209.

*Endrődi, G.*, 1979: Optimal evapotranspiration and rainfall for potato in Hungary (in Hungarian). *Beszámolók* 1977. Orsz. Meteorológiai Szolg., Budapest, 185-196.

*Endrődi, G.*, 1973: Investigation on water use of sugar beet (in Hungarian). *Beszámolók* 1970. Orsz. Meteorológiai Szolg., Budapest, 147-154.

*Endrődi, G.*, 1974: Agrometeorological basis of water demand and irrigation water need of sugar beet (in Hungarian). *Beszámolók* 1971. Orsz. Meteorológiai Sz., Budapest, 186-199.

*Erdős, L.*, 1966: Measurement of potential evapotranspiration (in Hungarian). *Időjárás 70*, 129-135.

*Fekete, L.* and *Szilágyi, T.*, 1979: Water use and phenometrical parameters of sweet corn (in Hungarian). *Beszámolók* 1977. Orsz. Meteorológiai Szolg., Budapest, 196-206.

*Huzulák, J.* and *Matejka, F.*, 1992: Stomatal resistance, leaf water potential and hydraulic resistance of sugar beet plants. *Biol. Plantarum 34*, 291-296.

*Kádár, F.* and *Szilágyi, T.*, 1980: Optimal evapotranspiration of maize, climatic water deficit and its yield (in Hungarian). *Beszámolók* 1978. Orsz. Meteorológiai Szolg., Budapest, 156-167.

*Kozma, F.* and *Füri, J.*, 1974: Evapotranspiration of grape (in Hungarian). *Beszámolók* 1971. Orsz. Meteorológiai Szolg., 215-226.

*Lawlor, D.W.* and *Milford, G.F.J.*, 1975: The control of water and carbon dioxide flux in water stressed sugar beet. *J. Exp. Bot. 26*, 657-665.

*Novák, J.* and *Szilágyi, T.*, 1980: Data for evapotranspiration of cucumber (in Hungarian). *Beszámolók* 1978. Orsz. Meteorológiai Szolg., Budapest, 199-210.

*Petrasovits, I.*, 1970: *Water Demand of Irrigated Plant Stands* (in Hungarian). Thesis, Hungarian Acad. Sci., Budapest.

*Posza, I.*, 1978: Effect of soil water depth on evapotranspiration (in Hungarian). *Beszámolók* 1975. Orsz. Meteorológiai Szolg., Budapest, 210-218.

*Posza, I.*, 1980: Evapotranspiration of canned vegetables (in Hungarian). *Beszámolók* 1978. Orsz. Meteorológiai Szolg., 226-232.

*Ruzsányi, L.*, 1975: *Investigation of Evapotranspiration of Plant Canopies at Different Nutrition Level* (in Hungarian). Ph.D. Thesis, Budapest.

*Ruzsányi, L.*, 1981: Influence of irrigation and fertilizers on yield and quality of sugar beet (in Hungarian). *Növénytermelés 30*, 363-370.

*Ruzsányi, L.*, 1990: Water demand of sugar beet and effect of irrigation (in Hungarian). *Növénytermelés 39*, 423-429.

*Stollár, A.* and *Gergely, I.*, 1978: Evapotranspiration of young apple trees (in Hungarian). *Beszámolók* 1976. Orsz. Meteorológiai Szolg., Budapest, 206-215.

*Szalóki, S.*, 1971: *Questions on Soil Water Level, Evapotranspiration and Irrigation* (in Hungarian). Ph.D. Thesis, Budapest.

*Szlovák, S.*, 1979: *Investigation on Transpiration and Evapotranspiration of Maize* (in Hungarian). Ph.D. Thesis, Budapest.

*Tóth, E.*, 1978: Evapotranspiration of maize at different levels of fertilizer and irrigation water (in Hungarian). *Beszámolók* 1975. Orsz. Meteorológiai Szolg., Budapest, 241-256.

*Walkowszki, A.*, 1978: Effect of plant density on maize evapotranspiration (in Hungarian). *Beszámolók* 1975. Orsz. Meteorológiai Szolg., Budapest, 256-260.

# IDŐJÁRÁS

*Quarterly Journal of the Hungarian Meteorological Service*
*Vol. 99, No. 1, January–March 1995*


## Simple analytic model of horizontal wind turning


**Ivica Vilibić**

*Hydrographic Institute of the Republic of Croatia,*
*Zrinsko-Frankopanska 161, 58000 Split, Croatia*



*(Manuscript received 3 October 1994; in final form 25 January 1995)*



**Abstract**—By assuming the linearity of the wind field and using data from two meteorological measuring stations, based on analytic relations, the model calculates the quantities which describe the horizontal wind turning and serve as input data for the transport and diffusion models. The model has been applied within the Gaussian model and the results obtained are satisfactory.



*Key-words:* wind field, transformation of coordinates, condensation factor, plume axis, application within a larger model.


### *1. Introduction*

Modeling of transport and diffusion processes in the atmosphere, sea and land play a very significant role nowadays. Industrialization and pollution of the Earth have produced the necessity of understanding and description of processes which take place on and inside it. To describe the atmospheric transport and diffusion processes on a mesoscale, Gaussian, K-, and Monte Carlo models are being applied successfully. Because of its analyticity, the Gaussian model is one of the most widely used models, but its limitation is that, because of irreal representation of the wind field, it is not able to describe the wind turning in the horizontal plane.

In this work a small contribution is given to the description of the horizontal turning of the smoke plume by using a set of simple analytic equations. It may be applied in orographically weakly developed regions where mesoscale horizontal wind turning occurs. Horizontal wind turning may be caused by the different roughnesses of the ground or urbanization in a region as well as by discontinuities between the water and dry land surfaces. Some descriptions about these problematics are shown in the article by *Šinik* (1982).

This model takes the coordinates $(x,y)$ of the place where concentration of the atmospheric constituents is wanted to be known and calculates the transformed coordinates $(x',y')$ and the condensation factor $e$, which describe the effects of wind turning and serve as input parameters for the transport and diffusion models. The wind field is modeled by the input data from two measuring meteorological stations (the simplest case), making use of the exponential law of the vertical variation of the wind speed and the linearization of the wind speed gradient. The assumptions of this model are chosen such that the transformation of coordinates may be described by analytic relations.

## *2. Input data. Wind field*

Input data of this model are the coordinates of two measuring meteorological stations as well as the speed and direction of wind at 10 meters above the ground, which are being measured by these stations. The domain can range between 10 and 100 square kilometers. We denote the coordinates of the two stations by $(x_1,y_1)$ and $(x_2,y_2)$ and assume that they are placed down the wind.

In such models it is often necessary to determine the wind at a certain height above the ground. To determine the wind speed at any height, exponential law of the vertical change of the wind speed (*Well* and *Brower*, 1984) can be used:

$$u_{1H} = u_1 \left( \frac{z}{10} \right)^p , \tag{1}$$

$$u_{2H} = u_2 \left( \frac{z}{10} \right)^p , \tag{2}$$

where $u_{1H}$ and $u_{2H}$ are the wind speeds at a height $z$ above the stations labelled 1 and 2, respectively, and $p$ is an exponent given by the relationships of the similarity theory (*Panofsky* and *Dutton*, 1984).

A schematic review of the turning of plume is given in *Fig. 1*. The distance from the source $I_s$ (which represents the plume source) to some point $(x_0,y_0)$ nearest to input point $(x,y)$ represents transformed coordinate $x'$, while transformed coordinate $y'$ is defined as the shortest distance from point $(x,y)$ to axis $x'$. The most general description of the turning of plume axis $x'$ in this model with two measuring stations assumes that the domain is divided into three regions.

*Region I* occupies the space from the source of emission to the station 1. Wind field is uniform and parallel to the $x$ axis, that is:

$$u = u_{1H}, \tag{3}$$

$$v = 0. \tag{4}$$

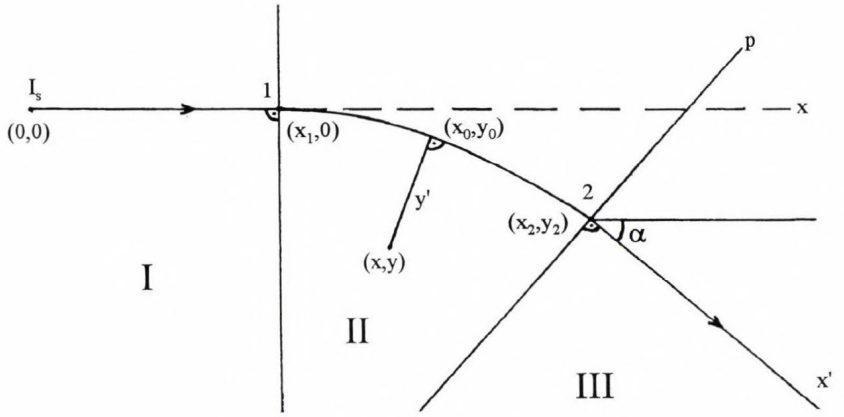


*Fig. 1.* Scheme of horizontal wind turning.

*Region II* represents the space of the plume turning, which is defined as a space between stations 1 and 2. It is assumed that the air flow turns it equally in the given region, so that the wind speed gradient in $y$-direction disappears, and that the same gradient in the $x$-direction is constant. Then, by expanding the wind field into a Taylor series, we can write it in this form:

$$u = u_{1H} + \frac{\partial u}{\partial x}(x - x_1) + \dots , \tag{5}$$

$$v = \frac{\partial v}{\partial x}(x - x_1) + \dots , \tag{6}$$

where the wind gradients are given by

$$\frac{\partial u}{\partial x} = \frac{u_{2H}\cos\alpha - u_{1H}}{x_2 - x_1} , \tag{7}$$

$$\frac{\partial v}{\partial x} = \frac{u_{2H}\sin\alpha}{x_2 - x_1} . \tag{8}$$

*Region III* represents the space away from station 2 where the direction of wind is parallel to the wind direction at this station, i.e.

$$u = u_{2H}\cos\alpha , \tag{9}$$

$$v = u_{2H}\sin\alpha . \tag{10}$$

## 3. *Mathematical formulation*

### *3.1 Region I*

In this region no wind turning occurs, so the transformation of coordinates and the condensation parameter can be described by the simple equations:

$$x' = x, \tag{11}$$

$$y' = y, \tag{12}$$

$$e = 1. \tag{13}$$

### *3.2 Region II*

In this region the plume turning occurs. By expanding into the Taylor series, and using Eqs. (5) and (6), components of the wind speed are

$$u = \frac{dx}{dt} = u_{1H} + \frac{\partial u}{\partial x}(x - x_1), \tag{14}$$

$$v = \frac{dy}{dt} = \frac{\partial v}{\partial x}(x - x_1), \tag{15}$$

where $\partial u/\partial x$ and $\partial v/\partial x$ are given by Eqs. (7) and (8). Equating $dt$ from Eqs. (14) and (15) and integrating, we obtain the trajectory of a particle in the plume axis or representation of the $x'$-axis in the $(x,y)$ coordinate system

$$y = b\left[x - x_1 - a \ln\left(1 + \frac{x - x_1}{a}\right)\right], \tag{16}$$

where

$$a = \frac{u_{1H}}{\partial u/\partial x}; \qquad b = \frac{\partial v/\partial x}{\partial u/\partial x}. \tag{17}$$

Relationship Eq. (15) and all further relations where $a$ and $b$ appear are valid if $\partial u/\partial x \neq 0$.

Determination of the coordinates $(x_0,y_0)$ which represent the nearest point to the input point $(x,y)$ on the plume axis $x'$ is based on calculating the coordinates of the intersection of curve (16) and the straight line determined by

points $(x_0,y_0)$ and $(x,y)$. Knowing the slope of the tangent at the plume axis at point $(x_0,y_0)$

$$k_t = \frac{b\,(x_0 - x_1)}{a + x_0 - x_1}, \tag{18}$$

we can establish the equation of the normal at the plume axis at $(x_0,y_0)$

$$y - y_0(x_0) = -\frac{a + x_0 - x_1}{b\,(x_0 - x_1)}\,(x - x_0), \tag{19}$$

from which $x_0$ may be calculated by iteration

$$x_0 = -\frac{y - y_0(x_0)}{x - x_0}\,(x_0 - x_1)\;b - a + x_1. \tag{20}$$

The arch length of the plume axis $x'$ from the point $x_1$ to a $x_0$ is given generally by

$$s(x_1,x_0) = \int_{x_0}^{x_1} \sqrt{1 + \left(\frac{dy}{dx}\right)^2}\,dx. \tag{21}$$

Applying Eq. (21) at Eq. (16) we would get a much more complicated relation, so in this work $s(x_1,x_0)$ is modeled by the 'trial-and-error' method (we assumed the form of equation and determine the parameters by 'adjusting') in the following way

$$s(x_1,x_0) = \frac{1}{\cos\dfrac{\alpha_0}{3.3}}\sqrt{(x_1 - x_0)^2 + y_0^2}, \tag{22}$$

where

$$\alpha_0 = arctg\frac{bx_0}{a + x_0}. \tag{23}$$

Using the quantities calculated above, the relations for transformation of coordinates $(x,y)$ into $(x',y')$ are given by

$$x' = x_1 + s(x_1, x_0)\,, \tag{24}$$

$$y' = \sqrt{(x - x_0)^2 + (y - y_0)^2}\,. \tag{25}$$

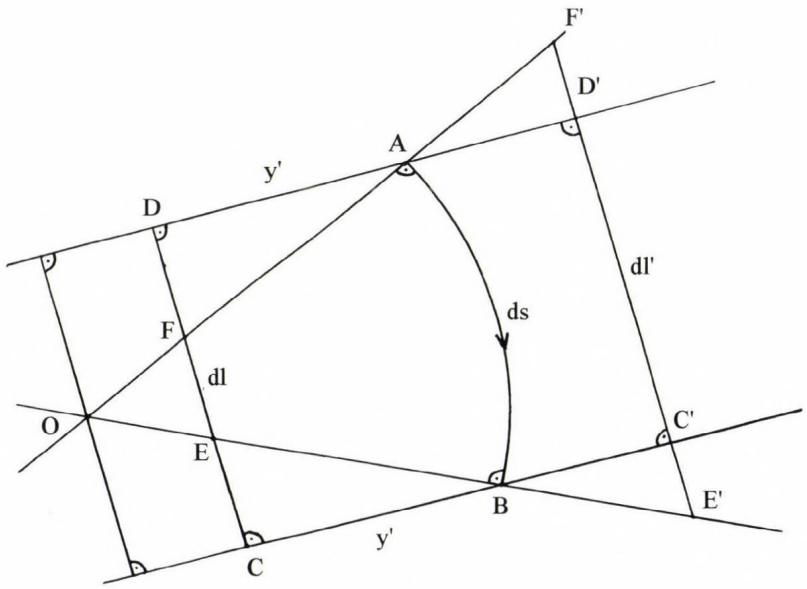


*Fig. 2.* Scheme of determining condensation factor.

The plume condensation factor $e$ is obtained by assuming that the condensation (or the dilution) equals the ratio of the areas of non-curved and curved plume (*Fig. 2*). Defining the plume axis by the arch AB, factor e is defined by the ratio of areas of the 'rectangle' ABCD ($dP_1$) and figure ABEF ($dP_2$) for the case of internal motion (concave part of domain), while for the case of external motion (convex part of domain) factor $e$ is defined by the ratio of areas of the figures ABC′D′ ($dP_1$) and ABE′F′ ($dP_2$)

$$e = \frac{dP_1}{dP_2}\,. \tag{26}$$

The area ABCD is given by

$$dP_1 \approx y'\, ds, \tag{27}$$

and ABEF by

$$dP_2 = \frac{1}{2} R\, ds - \frac{1}{2}(R - y')\, dl, \tag{28}$$

where $R$ represents the radius of plume axis curvature OA (or OB), which is mathematically defined by

$$R = \frac{\left[1 + \left(\frac{dy}{dx}\right)^2\right]^{3/2}}{\frac{d^2y}{dx^2}} \tag{29}$$

or substituting Eq. (16) into Eq. (29)

$$R = \left|\frac{a}{b}\right| \left(1 + \frac{x_0 - x_1}{a}\right)^2 \left[1 + \frac{b^2 (x_0 - x_1)^2}{(a + x_0 - x_1)^2}\right]^{3/2}. \tag{30}$$

The radius of curvature $R$ has been taken into account when modeling $e$ because of its excellent properties for description of turning of the plume axis.

Because $dl$ is infinitesimal, it may be calculated from the ratio of the similar triangle OAB and rectangle ABCD

$$dl = \frac{R - y'}{R}\, ds. \tag{31}$$

In the case when the input point $(x,y)$ is on the part of the region outside of the arc, i.e. if we consider the dilution, then the area ABE′F′ is

$$dP_2 = \frac{1}{2}(R + y')\ dl' - \frac{1}{2} R\ ds, \tag{32}$$

where $dl'$ is calculated from the triangles OE′F′ and OAB

$$dl' = \frac{R + y'}{R}\, ds, \tag{33}$$

while Eq. (26) is valid for $dP_1$. Putting relations (31) and (33) into (28) and (32), respectively, we become able to unify the calculation of $dP_2$ in both cases

$$dP_2 = \left[1 + \frac{1}{2}\frac{y'}{R} sgn\,(x - x_0)\right] y'\, ds, \tag{34}$$

where $x$ is input coordinate of the point, $x_0$ is the point given by relation (20), and *sgn* is sign function. It is obvious that for the internal part of the plume there is $x < x_0$ ($e < 1$) and for the external part there is $x > x_0$ (e > 1) (see Fig. 1).

Substituting Eqs. (34) and (27) into (26), the condensation factor $e$ is defined by

$$e = \frac{2R}{2R + y'\, sgn\,(x - x_0)}. \tag{35}$$

This relation does not hold in case $y'sgn\,(x - x_0) < -R$ because in that case the triangle OAB is completely contained in ABCD, so $e$ must be calculated by a linear extrapolation of the Eq. (35), accordingly

$$e = 1 - \frac{y'\, sgn\,(x - x_0)}{R}. \tag{36}$$

The complete set of equations for calculating $e$ in part II is

$$e = \frac{2R}{2R + y'\, sgn\,(x - x_0)}; \quad \text{if} \quad y'sgn\,(x - x_0) \geq -R$$

$$= 1 - \frac{y'sgn\,(x - x_0)}{R}; \quad \text{if} \quad y'sgn\,(x - x_0) < -R. \tag{37}$$

### *3.3 Region III*

In this region, which is separated from the previous one by the straight line $p$ (see Fig. 1)

$$p \equiv y - y_2 = -\frac{1}{tg\,\alpha}(x - x_2), \tag{38}$$

the plume is moving along a straight line so that

$$e = 1 \tag{39}$$

or, there is no plume condensation or dilutation.

Transformation of coordinates $x,y$ into $x',y'$ is made by using the following relations

$$x' = x_1 + s(x_1,x_2) + \sqrt{(x_v - x_2)^2 + (y_v - y_2)^2}, \tag{40}$$

$$y' = \sqrt{(x - x_v)^2 + (y - y_v)^2}, \tag{41}$$

where $(x_v,y_v)$ is the point on the plume axis nearest to the input point, and it is defined by

$$x_v = \frac{(y - y_2)\,tg\,\alpha + x_2(1 - tg^2\alpha)}{1 + tg^2\alpha}, \tag{42}$$

$$y_v = y - \frac{1}{tg\alpha}(x_v - x). \tag{43}$$

### *3.4 The case* $\alpha = 0$

All the equations given above (for the regions II and III) are defined for case $\alpha \neq 0$, while in case $\alpha = 0$, where there is no wind turning at all inside the whole domain, relations (11), (12) and (13) for the region I are used in whole domain.

### *3.5 The case* $\partial u/\partial x = 0$

If the gradient of wind along $x$ happens to disappear, which means $u_{2H}\cos\alpha = u_{1H}$, then the parameters $a$ and $b$ become infinite. That is why we have to reformulate the relations where $\partial u/\partial x$, $a$ and $b$ appear.

The Taylor expansion of relation (4) is in this case

$$u = u_{1H} = \frac{dx}{dt}, \tag{44}$$

$$v = \frac{\partial v}{\partial x}(x - x_1) = \frac{dy}{dt}, \tag{45}$$

from which we derive equation of the plume axis in region II

$$y = \frac{1}{u_{1H}} \frac{\partial v}{\partial x} \frac{(x - x_1)^2}{2}. \tag{44}$$

Relationship (22) turns into

$$s(x_1,x_0) = \frac{1}{2}\left[(x - x_1)\sqrt{1 + \left[\frac{1}{u_1}\frac{\partial v}{\partial x}(x - x_1)\right]^2} + \frac{u_1}{\partial v/\partial x} Arsh\left[\frac{1}{u_1}\frac{\partial v}{\partial x}(x - x_1)\right]\right], \tag{45}$$

while formula (30) is transformed into

$$R = \frac{u_1}{\partial v/\partial x}\left[1 + \left[\frac{1}{u_1}\frac{\partial v}{\partial x}(x - x_1)\right]^2\right]^{3/2}.$$

In this way all the possibilities of occurrence of the wind field are defined, so turning of the plume axis is defined for all the combinations of input parameters where $|\alpha| < 90°$ holds. By calculating the transformed coordinates $x',y'$ and the condensation factor $e$, we obtain the complete definition of parameters needed when applying various transport and diffusion models (one of which is the Gaussian model).

## *4. Application and results*

This model has been applied within the Gaussian transport and diffusion model for continuous sources, where it has served to describe spreading of pollutants in the planetary boundary layer. The distribution of concentrations obtained by the Gaussian model has given a fairly good description of the spreading of pollutants in the atmosphere, taking into account the horizontal turning of the plume. Some results (for unstable, neutral and stable atmosphere, respectively) are shown in *Fig. 3* for constituent $SO_2$. Horizontal distance between two nearest points (circles) are 500 meters and the area of the circle is proportional to the concentration of pollutants. Wind direction in the first 3000 meters is parallel two the $x$ axis, from 3000 meters it continuously turns towards angle of 45 degrees at distance 8000 m, and further it does not vary. It is observed that the condensation factor $e$ has a small effect in the region near the plume axis (where the largest concentrations occur) and it is approximately equal to 1, while at largest distances from the plume axis the effect of it becomes bigger. Because of the smaller concentrations than inside the plume axis, its total effects are quite small.

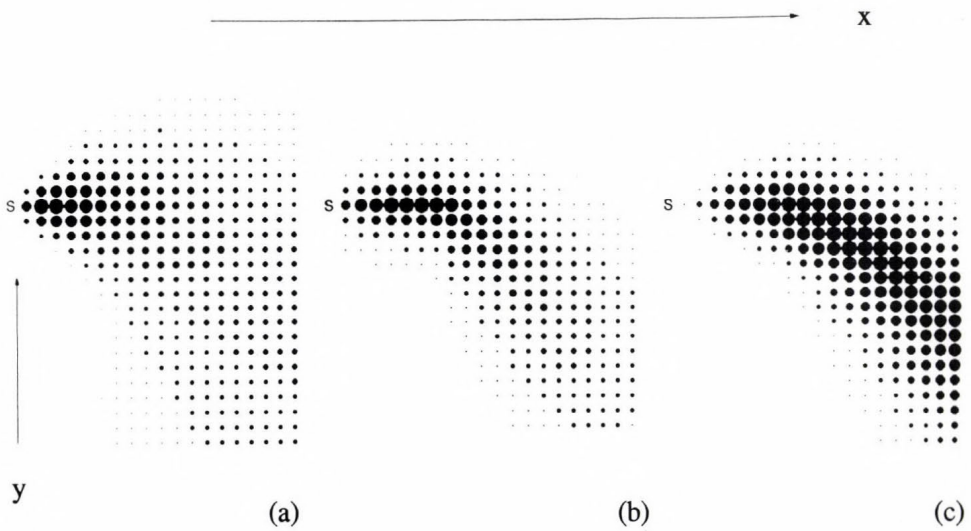


*Fig. 3.* Spreading of pollutants in (*a*) unstable, (*b*) neutral, and (*c*) stable atmosphere. *S:* source of pollutant emission.

## 5. Conclusion

The simple analytic model of horizontal wind turning is applicable within the larger models which describe the transport and diffusion processes of atmospheric constituents. Based on the input data of the speed and direction of wind and the positions of two measuring meteorological stations the wind field is described by analytic equations within the whole considered region. By mathematical procedures we obtain the trajectory of constituents of the atmosphere in the plume centre (axis), the transformed coordinates which represent the distance from the observed point to the plume axis, and also the distance of the constituents transport on the plume axis.

The condensation factor is also defined which describes condensation (or dilution) of the plume depending on the $x'$ axis turning and input coordinates of the points. These quantities represent input parameters for the transport and diffusion models, for example the Gaussian plume model, which uses the trajectories obtained by this model for calculating the transport of atmospheric constituents.

Further extensions of this model are possible if we include more than two measuring stations and also by taking into account the vertical component of the wind field induced by the orography. To describe the wind field the objective analysis method may be used, as well. Such representation would not be analytic, because we would have to apply numerical methods.

**Acknowledgements**—I wish to thank *Mr. Nadežda Šinik* for his unselfish advices while the model was being built up. Also I thank *Artic Sergio* for giving computer support and *Ljerka Zekanovic* for lectoring the article.

## References

*Panofsky, H.A.* and *Dutton, J.A.*, 1984: *Atmospheric Turbulence*. John Wiley & Sons, New York, 397 pp.

*Šinik, N.*, 1982: Mesoscale variation of average airflow in application to time integrated concentration Gaussian models. *Atmos. Environ. 16*, 2061-2069.

*Well, J.C.* and *Brower, R.P.*, 1984: Un updated Gaussian plume model for tall stacks. *JAPCA 34*, 818-827.

# BOOK REVIEW

*Ian N. James*: **Introduction to Circulating Atmospheres**. Cambridge Atmospheric and Space Science Series, Cambridge University Press, 1994, Cambridge, 422 numbered pages, numerous figures.

This book is one of the Cambridge Atmospheric and Space Science Series. It was born from the expansion of university courses that the author gave on the topic of atmospheric circulation. In the preface the author addresses his book to students familiar with the basic concepts of atmospheric dynamics at an introductory university level and researchers who are research interested in the atmospheric circulation. However, this book is undoubtedly more than a simple coursebook. It is a well-rounded, thorough text that strikes a nice balance between mathematical theory and meteorological interpretation. The book consists of ten chapters. 1. The governing physical laws. 2. Observing and modelling of global circulation. 3. The atmospheric heat engine. 4. The zonal mean meridional circulation. 5. Transient disturbances in the midlatitudes. 6. Wave propagation and steady eddies. 7. Three-dimensional aspects of the global circulation. 8. Low frequency variability of the circulation. 9. The stratosphere. 10. Planetary atmospheres and other fluid systems.

Chapters 1 to 7 summarize the classical theory of the atmospheric circulation and present a large amount of figures and maps based on atmospheric observations. A large part of the observed data used in this book has been analyzed at the European Centre for Medium Range Weather Forecasts. Quite a large amount of new data have been analyzed and the author's scientific activity up till now guaranties the outstanding quality of analysis techniques. This feature makes this book the most valuable and up-to-date collection of figures on the topic of atmospheric circulation. In these chapters Dr. James has not made an attempt to write a review of the state-of-art literature on the atmospheric circulation. Indeed, he makes an effort to present the simplest conceptual (and mathematical) models of the phenomena which are in good accordance with the observations, thus avoiding the use of much more sophisticated mathematics of recent studies, unless they provide a substantially better theoretical approach. A good example of this attempt is the description of the theory of baroclinic instabilities by the simple but really adequate Eady model.

An additional outstanding feature of this book is the strict distinction between the notion of Lagrangian and Eulerian atmospheric circulations. Most of the previous textbooks have not dealt in details with the Lagrangian circulation. Moreover, they have not emphasized the differences between the two approaches, although the realization of these differences had led to the

exact understanding of the Eulerian circulation in the upper troposphere and the stratosphere. This fact makes this text an excellent first book on atmospheric dynamics for researchers in the field of large scale atmospheric transport processes. This statement is especially valid taking into consideration that Chapter 9 gives a detailed description of the circulation of the stratosphere, which plays much more important role in the transport processes than it was thought earlier.

While the above-mentioned Chapter 9 gives an overview of the present knowledge of stratospheric circulation, in Chapter 8 the variability of circulation is presented on the base of the theory of dynamical systems. This chapter makes the book an up-to-date textbook on the atmospheric circulation of the Earth, while Chapter 10 makes it a complete textbook on circulating atmospheres. This last chapter discusses the planetary atmospheres on the simple but fruitful realization that terrestrial circulation is only one of the possible circulations. What specifies circulating atmospheres, is the geometrical properties of the motions of planets: radius of the planet, speed of rotation (Coriolis parameter), distance from the Sun (solar constant). The text in the first seven sections is organized in a way, that changing the above parameters readers can get a detailed description of the dynamics of any planetary atmospheres. It is really interesting to see that the Eady model of baroclinic instabilities works for other planets, not only for the Earth. One subsection deals with Saturn's moon Titan, which has a stick atmosphere in which prebiotic complex organic solids form and fall down onto the surface.

This book constitutes an up-to-date overview of circulating atmospheres. Because of its relative simplicity and plenty of carefully analyzed data it will serve as a valuable reference volume to researchers in the filed of dynamic meteorology and climatology.

*I. Szunyogh*

# NEWS

## In memoriam J. Kakas
(1909–1994)

*Dr. József Kakas*, the well-known Hungarian classical climatologist, died on 4 October 1994. He was, among other charges, the Editor of the journal *Időjárás* between the years 1953 and 1968. He did this job with a high-level scientific and technical competence. Even as a retired scientist he participated in the editional work until 1990.

J. Kakas was born on 31 July 1909 in Zalaegerszeg. He attended a monastic secondary school (S.P.) in Nagykanizsa where he sat for the final examination in 1928. He took the master's degree in geography and history at the Pázmány Péter University of Budapest. He entered service of the Hungarian Meteorological Institute in 1937. His first research area was the investigation of precipitation and humidity distributions in Hungary as well as the study of wind climatology of the country. In some years he became an excellent climatologist approaching the atmospheric processes from the viewpoint of geography. The results of his research were published in several papers and books in the fifties. On the basis of natural criteria, he established new climatic regions in Hungary. Appreciating his scientific activity the Hungarian Academy of Sciences awarded him the degree of Ph. D. in 1962.

Dr. Kakas was appointed the head of the Department of Climatology of the Institute in 1953 and he became the chief of the Division of Climatology and Hydrology in 1963. In this period he directed the so-called Balaton Project aiming to reveal the climatology of the lake. This Project resulted in more than hundred publications prepared by the scientists involved. J. Kakas retired after a long and successful carrier in 1971. However, even after his retirement, he edited a book entitled *The Climate of Balaton* which was published in 1974 by the Hungarian Meteorological Service. In this volume the authors analyse and discuss the climatic, radiative, energetic and hydrological systems and other peculiarities of Lake Balaton. In addition to the work of *L. Lóczy* and *J. Cholnoky* at the beginning of the 20th century this is the most detailed scientific monograph about the lake.

An outstanding editorial achievement of J. Kakas was the Climate Atlas of Hungary published in 1960 and also a second volume of this publication containing detailed climatic data of the country. The success of his efforts is well demonstrated by the fact that, for the Climate Atlas of Europe published by the World Meteorological Organisation, the maps of the distribution of several climatic elements were prepared by a Hungarian working group headed

by him. After a careful working of several years the Atlas was issued in 1970 and had a great success.

The determining feature of the life of Dr. Kakas was the accurate, conscientious and correct work. Several meteorologists of the rising generation, inherited these qualities from him.

The memory of József Kakas will forever remain in the hearts of his friends working in the fields of meteorology, geography and hydrology.

*M. Kéri*

## Scientific Days '94 on Meteorology

The traditional annual Scientific Days on Meteorology were organized by the Scientific Committee on Meteorology of the Earth Sciences Class of the Hungarian Academy of Sciences and the Hungarian Meteorological Service (HMS) in the Center of the Federal Chamber of Technical and Scientific Societies in Budapest on 17th and 18th November 1994. The subject of the program was weather forecasting. In the frame of three sessions altogether 21 papers were presented. Because of the large number of presentations 5 contributions were exhibited as poster.

The program was introduced by two foreign authors' papers (*J.-F. Geleyn*, Météo-France and *J. McGinley*, NOAA, FSL), moreover, in the compilation of additional 5 papers also foreign, American, French and Swiss scientists as co-authors took part. Among the Hungarian lecturers, even scientists from the Water Resources Research Center (VITUKI) and the Meteorological Department of Eötvös Loránd University (MD-ELTE) should be mentioned. Further, the presentations are shortly shown but the name of only the speaker of the authors is given.

*J.-F. Geleyn* talked about ALADIN project brought into existence by French proposal. The ALADIN is a fine mesh variant of the ARPEGE model for Central and Eastern Europe. Presently, the model is run in Toulouse and the output is transmitted to the users by satellite. *J. McGinley* gave information about activity of local weather offices in U.S.A., amounting to 150. During the last ten years the available weather information was about tripled. The LAPS (Local Analysis and Prediction System) developed in FSL enables to display gridded weather data (from surface, satellite, radar and aircraft) to the forecasters. *G. Götz* studied the problem of predictability on the basis of the chaos theory. He pointed out the high sensitivity to the initial conditions which defines a theoretical limit to the predictability. Furthermore, he informed about methodological bases of the ensemble forecasts overtaking this difficulty. *I. Szunyogh* delivered two papers about the results of common researches carried out together co-workers of NMC. In the first one local stability parameters

were presented through some examples. The Arnold method was concerned which is capable of examining only stationary solutions of adiabatic models. The other paper dealt with problems of optimal perturbations. A numerical experiment series was shown in which the optical perturbations were performed by two varieties of medium range model used in NMC.

A global spectral shallow water model developed in NCAR was adapted at MD-ELTE into which the topographical effect was incorporated. In the attempts carried out with the model the sensitivity of the model and unstable perturbations to the topography was investigated (*B. Kádár*). The formation and dynamics of frontal waves, so important in view of weather forecasting, were studied in the paper by *A. Horányi*. He wanted to discover which factors in the initial conditions are favorable to the formation and development of waves. The attempts were implemented by adjoint application of ARPEGE/ALADIN model.

As known, in numerical weather prediction models based on primitive equations the filtration of gravitational waves is necessary. *G. Radnóti* presented an initialization method and searched for the effectivity of the recursive and non-recursive filters and the interaction of the dissipative forcings and filtering. In another paper it was studied how the covariance of forecast errors could be derived (*D. Dévényi*). He examined, by using one- and two-level models and statistical characteristics of them, how the errors, both being in the initial conditions and resulting from the approaching feature of the model, developed during the forecasting period. In addition to weather forecasting the climate prognosis was also included in the program of the session. In order to obtain expectable regional climate changes a medium resolution meso-scale model was embedded into T42 variant of GCM (*J. Bartholy*), and the orography and roughness of the surface were also incorporated. In this way she succeeded in reconstructing the historical data series and estimating the temperature and precipitation scenarios related to $CO_2$ doubling.

*Á. Horváth* talked about recently installed workstation of the forecasting service, pointing out main functions of it: spatial and temporal data assimilation (e.g. use of uniform map projection), preparation of spatial and temporal cross-sections, complete data handling. The newest variant (ITTP 4.02 model) of the program extracting atmospheric profiles from TOVS data by NOAA is available in HMS. *É. Borbás'* paper presented an intercomparison study of the data which were produced by satellite and radiosondes, and prediction model.

The last, third session was devoted to the subject of operational forecasting. *Á. Takács* informed about the forecasting activity carried out as a duty obliged to the state. This presentation was closely connected with the next paper given by *M. Sallai* about the work of the aviation meteorological center of the HMS. In addition to servicing the international airlines the performance of requirements of private flights plays an increasing role. In summer time a storm warning service is operating at Lake Balaton. A decisive technique was developed for forecasting the storms associated with convective systems (*Á. Zsikla*).

*G. Csima* rendered account of Hungarian experiences in connection with application of one-month forecasting method developed by the UK Meteorological Office. After then two papers were presented by co-workers of VITUKI. Both authors (*P. Bartha* and *G. Bálint*) emphasized the importance of meteorological forecasts in the hydrological activity. Because of stratospheric ozone depletion the claim to forecast UV-B radiation is increasing. A work showed that the intensity of UV-B radiation depends in high degree on the weather conditions as well, and forecasting may be made only taking into consideration both the ozone content and the weather situation (*P. Németh*).

At the end of the session two reports were given about the utilization of weather forecasts (*M. Bóna* and *A. Maller*). They informed about both the result of a public opinion test related to the forecasts and the distribution of the claims with respect to the users. The special forecast products could be ranged into four groups: medical meteorology, protection of environment, warning and informing the media.

The posters were concerned with very various topics; just in some words: Regionalization of global climate prediction (*J. Bartholy et al.*), Cloud classification by cluster analysis (*M. Diószeghy*), Forecasting for sport flights by using GRID and TEMP data (*A. Fövényi*), Estimation of rainfall efficiency by combined analysis of radar and satellite information (*J. Kerényi*), A warning system for water quality of Danube (*G. Pintér*, VITUKI).

*T. Tänczer*

# ATMOSPHERIC ENVIRONMENT

an international journal

To promote the distribution of Atmospheric Environment *Időjárás* publishes regularly the *contents* of this important journal. For further information the interested reader is asked to contact *Dr. P. Brimblecombe,* School for Environmental Sciences, University of East Anglia, Norwich NR 7TJ, U.K.

## Volume 28 Number 20 1994



## Volume 28 Number 21 1994

## Volume 28 Number 22 1994

### *The Indoor Air '93 Congress*



*Regular Papers*

*P.M. Haygarth, D. Fowler, S. Stürup, B.M. Davison* and *K.C. Jones:* Determination of gaseous and particulate selenium over a rural grassland in the U.K., 3655-3663.

*A. Venkatram, P. Karamchandani, P. Pai* and *R. Goldstein:* The development and application of a simplified ozone modeling system (SOMS), 3665-3678.

*L.A. DE P. Vasconcelos, E.S. Macias* and *W.H. White:* Aerosol composition as a function of haze and humidity levels in the southwestern U.S., 3679-3691.

## Volume 29 Number 1 1995

*F. Maupetit, D. Wagenbach, P. Weddeling* and *R.J. Delmas:* Seasonal fluxes major ions to a high altitude cold alpine glacier, 1-9.

*J.E. Sloof:* Lichens as quantitative biomonitors for atmospheric trace-element deposition, using transplants, 11-20.

*Y. Muramatsu* and *S. Yoshida:* Volatilization of methyl iodide from the soil-plant ssytem, 21-25.

*L.W. Richards:* Airborne chemical measurements in nighttime stratus clouds in the Los Angeles Basin, 27-46.

*G. Petersen, Å. Iverfeldt* and *J. Munthe:* Atmospheric mercury species over Central and Northern Europe. Model calculations and comparison with observations from the Nordic Air and Precipitation Network for 1987 and 1988, 47-67.

*M.J. Hammond, C.S. Mill, D. Lacey, R.I. MacKay, T.W. Choularton, M.W. Gallagher* and *K.M. Beswick:* A fast-response multi-pass transmissometer operating over variable wavelength ranges, 69-76.

*P. Kirkitsos* and *D. Sikiotis:* Deterioration of Pentelic marble, Portland limestone and Baumberger sandstone in laboratory exposures to gaseous nitric acid, 77-86.

*S. Galmarini, J. Vilà-Guerau de Arellano* and *P.G. Duynkerke:* The effect of micro-scale turbulence on the reaction rate in a chemically reactive plume, 87-95.

*N. Yamamoto, H. Nishiura, T. Honjo, Y. Ishikawa* and *K. Suzuki:* A long-term study of atmospheric ammonia and particulate ammonium concentrations in Yokohama, Japan, 97-103.

*D.W. Byun* and *R. Dennis:* Design artifacts in Eulerian air quality models: evaluation of the effects of layer thickness and vertical profile correction on surface ozone concentrations, 105-126.

*H.A. Khwaja:* Atmospheric concentrations of carboxylic acids and related compounds at a semiurban site, 127-139.

## Volume 29 Number 2 1995

*S.R. Dorling* and *T.D. Davies:* Extending cluster analysis-synoptic meteorology links to characterise chemical climates at six northwest European monitoring stations, 145-167.

*F.J. Comes, W. Armerding, M. Spiekermann, J. Walter* and *Chr. Rüger:* Point measurements of tropospheric trace gases at Tenerife by a laser absorption technique, 169-174.

*K. Bächmann, I. Haag* and *K. Steigerwald:* Determination of transition metals in size-classified rain samples by atomic absorption spectrometry, 175-177.

*N.E. Peters* and *R.S. Reese:* Variations of weekly atmospheric deposition for multiple collectors at a site on the shore of Lake Okeechobee, Florida, 179-187.

*L.K. Peters, C.M. Berkowitz. G.R. Carmichael, R.C. Easter, G. Fairweather, S.J. Ghan, J.M. Hales, L.R. Leung, W.R. Pennell, F.A. Potra, R.D. Saylor* and *T.T. Tsang:* The current state and future direction of Eulerian models in simulating the tropospheric chemistry and transport of trace species: a review, 189-222.

*D.H.F. Atkins* and *D.S. Lee:* Spatial and temporal variation of rural nitrogen dioxide concentrations across the United Kingdom, 223-239.

*H. Horvath:* Estimation of the average visibility in central Europe, 241-246.

## Volume 29 Number 3 1995

# NOTES TO CONTRIBUTORS

The purpose of *Időjárás* is to publish papers in the field of theoretical and applied meteorology. These may be reports on new results of scientific investigations, critical review articles summarizing current problems in certain subject, or shorter contributions dealing with a specific question. Authors may be of any nationality but papers are published only in English.

Papers will be subjected to constructive criticism by unidentified referees.

* * *

The manuscript should meet the following formal requirements:

*Title* should contain the title of the paper, the names(s) of the author(s) with indication of the name and address of employment.

The title should be followed by an *abstract* containing the aim, method and conclusions of the scientific investigation. After the abstract, the *key-words* of the content of the paper must be given.

*Three copies* of the manuscript, typed with double space, should be sent to the Editor-in-Chief: *P.O. Box 39, H-1675 Budapest,* Hungary.

*References:* The text citation should contain the name(s) of the author(s) in Italic letter or underlined and the year of publication. In case of one author: *Miller* (1989), or if the name of the author cannot be fitted into the text: *(Miller,* 1989); in the case of two authors: *Gamov* and *Cleveland* (1973); if there are more than two authors: *Smith et al.* (1990). When referring to several papers published in the same year by the same author, the year of publication should be followed by letters a,b etc. At the end of the paper the list of references should be arranged alphabetically. For an article: the name(s) of author(s) in Italics or underlined, year, title of article, name of journal, volume number (the latter two in Italics or underlined) and pages. E.g. *Nathan, K. K.,* 1986: A note on the relationship between photosynthetically active radiation and cloud amount. *Időjárás 90,* 10-13. For a book: the name(s) of author(s), year, title of the book (all in Italics or underlined with except of the year), publisher and place of publication. E.g. *Junge, C. E.,* 1963: *Air Chemistry and Radioactivity.* Academic Press, New York and London.

*Figures* should be prepared entirely in black India ink upon transparent paper or copied by a good quality copier. A series of figures should be attached to each copy of the manuscript. The legends of figures should be given on a separate sheet. Photographs of good quality may be provided in black and white.

*Tables* should be marked by Arabic numbers and provided on separate sheets together with relevant captions. In one table the column number is maximum 13 if possible. One column should not contain more than five characters.

*Mathematical formulas* and *symbols:* non-Latin letters and hand-written marks should be explained by making marginal notes in pencil.

The final text should be submitted both in manuscript form and on *diskette.* Use standard 3.5" or 5.25" DOS formatted diskettes for this purpose. The following word processors are supported: WordPerfect 5.1, WordPerfect for Windows 5.1, Microsoft Word 5.5, Microsoft Word 6.0. In all other cases the preferred text format is ASCII.

* * *

Authors receive 30 *reprints* free of charge. Additional reprints may be ordered at the authors' expense when sending back the proofs to the Editorial Office.

Published by the Hungarian Meteorological Service

Budapest, Hungary

**INDEX: 26 361**

**HU ISSN 0324-6329**